

Ostracods and rock facies associated with the Devonian-Carboniferous boundary series in the Puech de la Suque section, Montagne Noire, France

by Jean-Georges CASIER, Francis LETHIERS & Alain PRÉAT

CASIER, J.-G., LETHIERS, F. & PRÉAT, A., 2001. – Ostracods and rock facies associated with the Devonian-Carboniferous boundary series in the Puech de la Suque section, Montagne Noire, France. *Bulletin de l'Institut royal des Sciences naturelles de Belgique, Sciences de la Terre*, 71: 31-52, 8 pls., 2 figs., 1 table, Bruxelles-Brussel, May 15, 2001. – ISSN 0374-6291.

Abstract

4,750 ostracods valves and carapaces have been extracted from across the Devonian-Carboniferous boundary sequence in the Puech de la Suque section, Montagne Noire, southern France, and 72 species have been identified half of which belong to the Thuringian ecotype. The study revealed that a maximum of 31.5 percent of the species disappeared in this section as a result of the Hangenberg Event — a low rate of extinction compared to that generally associated worldwide with the Frasnian-Famennian boundary (75 %). The Hangenberg Event differs also from the Frasnian-Famennian boundary Event by the absence of ostracod “disaster species”.

The facies of the boundary series is relatively homogeneous and composed of grey to slightly pinkish and yellowish mudstones and wackestones with various bioclasts (ammonoids, trilobites, bivalves etc.), and radiolarian wackestones and packstones. Despite the difficulty to reconstruct a bathymetric profile, the inferred environment points to quiet and deeper water-conditions, below or near the storm wave base, and there is no evidence of turbidites and mudflows. The succession corresponds most likely to a distal carbonate ramp, its lower part being characterized by hemipelagic or pelagic sediments. The microfacies analysis shows that no significant paleo-environmental changes occurred at the Devonian-Carboniferous boundary.

Two new species (*Proparaparchites?* *procerus* nov. sp. and *Paraparchites puechdelasuquensis* nov. sp.), and one new sub-species (*Gerodia weyeri olempskae* nov. subsp.) are established.

Key-words: Ostracods - Sedimentology - Devonian-Carboniferous boundary - Hangenberg Event - Montagne Noire

Résumé

4750 valves et carapaces d'ostracodes ont été extraites de part et d'autre de la limite Dévonien-Carbonifère, dans la coupe du Puech de la Suque (Montagne Noire, France) et 72 espèces sont identifiées dont la moitié appartient à l'écotype de Thuringe. L'étude montre qu'un maximum de 31,5 pour-cent des espèces d'ostracodes disparaissent suite à l'Événement Hangenberg, valeur faible en comparaison de l'extinction (75 %) observée à la limite des étages Frasnien et Famennien. L'Événement Hangenberg diffère aussi de celui de la limite Frasnien-Famennien, par l'absence d'espèces d'ostracodes profuseuses.

Les faciès observés sont homogènes et composés de mudstones et wackestones gris légèrement rosâtres ou jaunâtres, à bioclastes variés (ammonoides, trilobites, bivalves...), et de wackestones et packstones à radiolaires. Malgré la difficulté d'établir une courbe bathymétrique, l'environnement correspondant était calme et profond, situé sous ou à proximité du niveau d'action des vagues de tempêtes, sans la présence de turbidites et de courants de boue. La succession correspond à une rampe carbonatée distale, dont la partie inférieure est caractérisée par une sédimentation hémipelagique ou pélagique.

L'analyse des microfaciès montre qu'il n'y a pas de changement important de l'environnement au niveau de la limite Dévonien-Carbonifère.

Deux nouvelles espèces (*Proparaparchites?* *procerus* nov. sp. et *Paraparchites puechdelasuquensis* nov. sp.) et une nouvelle sous-espèce (*Gerodia weyeri olempskae* nov. subsp.) sont fondées.

Mots-clefs: Ostracodes - Sédimentologie - Limite Dévonien-Carbonifère - Événement Hangenberg - Montagne Noire

Introduction

Several “extraordinary” events are recorded from the late Devonian (HOUSE, 1985; WALLISER, 1984, 1996, HALLAM & WIGNALL, 1997) — among them the famous Hangenberg Event of central Europe close to the Devonian-Carboniferous boundary. This event, also called the Final Devonian Event or the D-C Boundary Event, corresponds to the deposition of the Hangenberg Shale in the Middle *praesulcata* Zone — the penultimate conodont zone in the Famennian. This dark-grey lithologic unit, recognized in many regions of the world, has been named by SCHMIDT (1924) after a locality in the Rheinische Schiefergebirge of Germany (WALLISER, 1984). The most conspicuous changes linked to this event happened within the ammonoids (HOUSE, 1993; R.T. BECKER, 1993), but noteworthy changes occurred also within the conodonts (GIRARD, 1996) and trilobites (FEIST, 1991). WALLISER (1996) noticed also that pelagic and hemipelagic faunas were more strongly influenced than neritic shallow-water faunas. The Hangenberg horizon is frequently ascribed to anoxic water conditions (HOUSE, 1985; BECKER & BLUMENSTENGEL, 1995), to a climatic cooling episode (CAPLAN & BUSTIN, 1999), or even to abnormal salinity conditions (FEIST & FLAJS, 1987).

The goal of this paper is to document the influence of the Hangenberg Event on the distribution of ostracods in the Puech de la Suque section (Montagne Noire, southern France), selected for the excellent exposure of upper Famennian and lower Tournaisian sequences, and for its notable richness in ostracods.

The Puech de la Suque section - General setting

The Puech de la Suque section (N43°29'934; E3°5'930) is located on the south-eastern slope of the Puech de la Suque Hill, 1.8 km south-east from St. Nazaire-de-

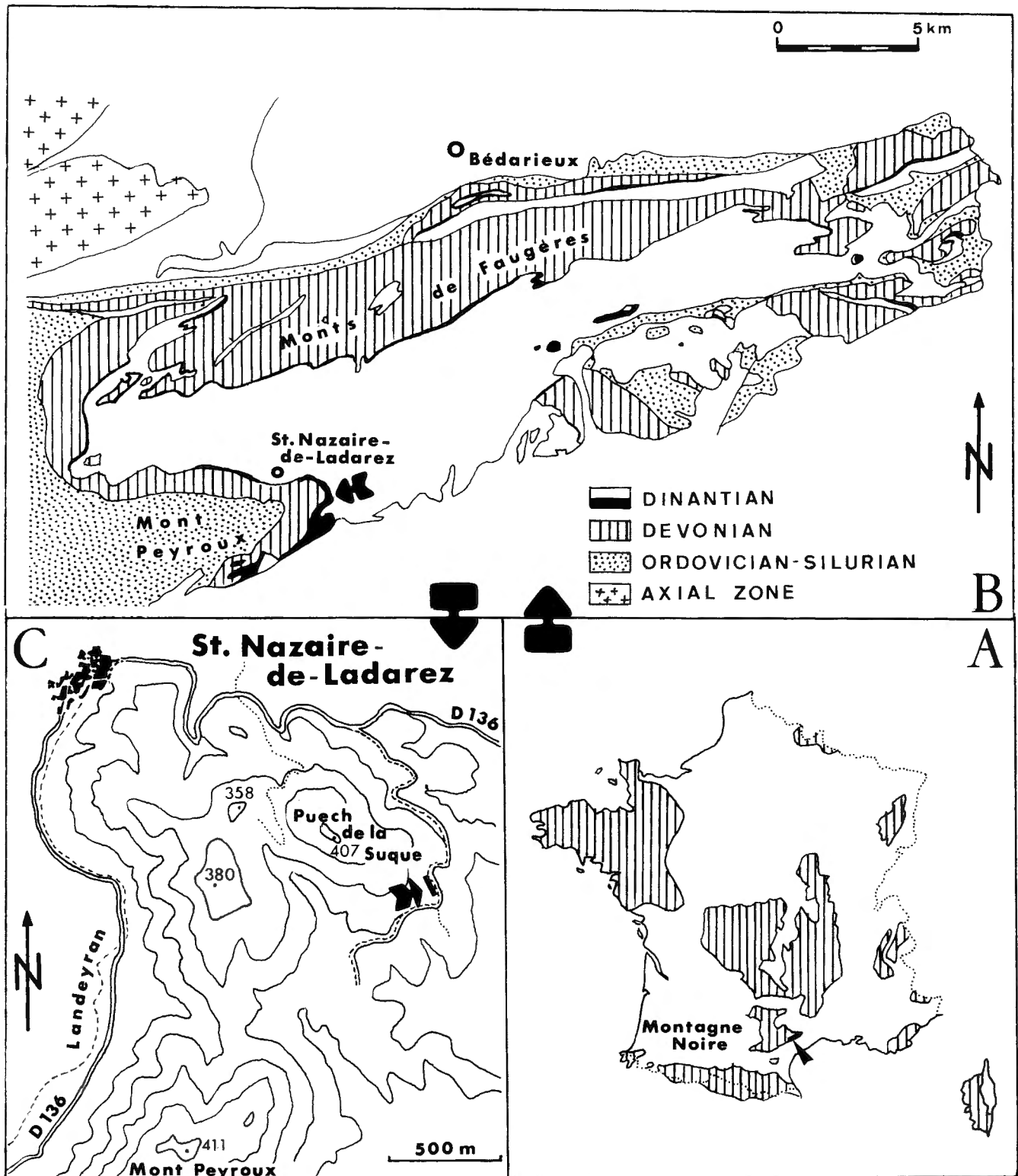


Fig. 1 — Geographic location of the Puech de la Suque section. A. Location of the Montagne Noire among the French Paleozoic outcrop belt. B. Detailed maps of the south-eastern part of the Montagne Noire. C. Locations of the Puech de la Suque and of the studied section (after LETHIERS & FEIST, 1991).

Ladarez (Fig. 1). The section has been studied by BOYER *et al.* (1968), MICHEL (1981), BECKER *et al.* in FEIST ed. (1990), and LETHIERS & FEIST (1991). The section investigated (Fig. 2) includes the middle and upper members of the so-called "Griotte Limestone Formation" interrupted

by a 25 cm thick dark grey silty shale bed, the Hangenberg horizon (FEIST, 1985), containing very thin (0.5 cm), reddish, nodular carbonate intercalations. The first bed on top of the Hangenberg horizon contains exclusively Protognathotid conodonts, whereas *Siphon-*

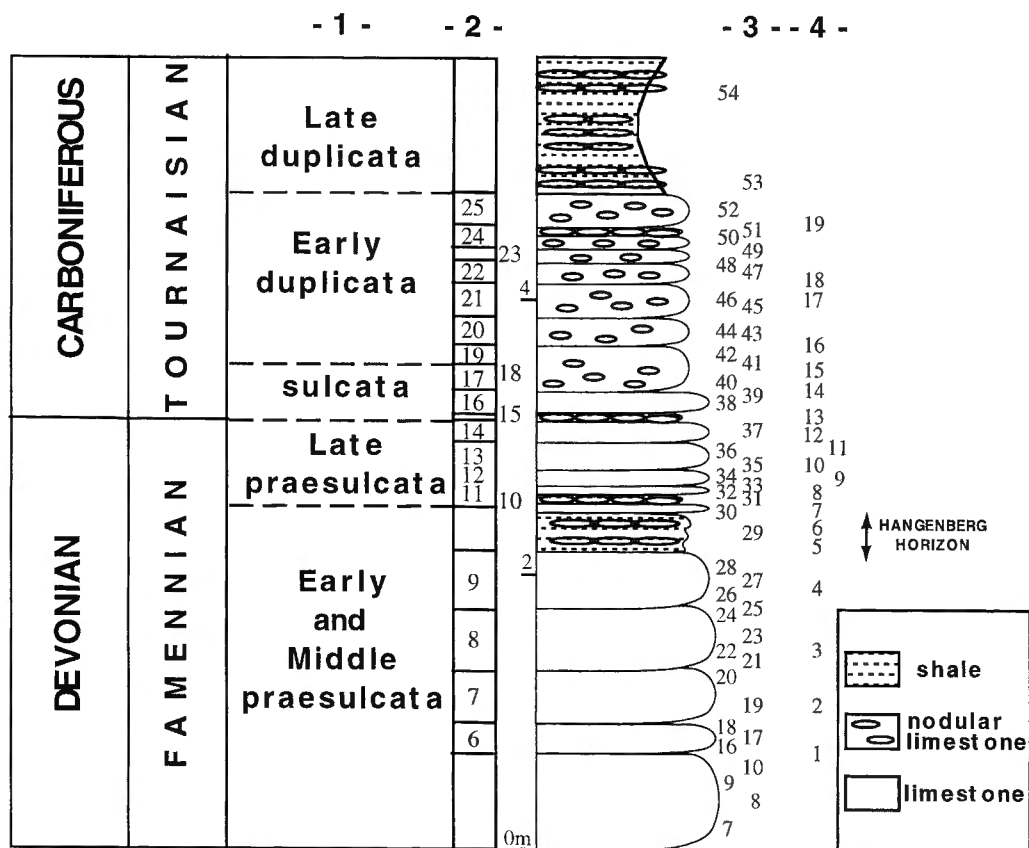


Fig. 2 — Lithological column of the Puech de la Suque section and position of sedimentological (3) and ostracod samples (4). Conodont zonation (1) and number of beds (2) after R. T. BECKER *et al.* (*in FEIST ed.*, 1990) & GIRARD (1996).

nodella sulcata first occurs in bed 15 of FEIST (*Ibid.*) where the Devonian-Carboniferous boundary is drawn (GIRARD, 1996). Structurally the Puech de la Suque section is overturned.

Rock and facies analysis (A. Préat)

The facies of this well-bedded boundary series (Fig. 2) is relatively homogeneous and composed of grey to slightly pinkish and yellowish mudstones and wackestones with various bioclasts (ammonoids, trilobites, bivalves, ostracods, crinoids, and rare bryozoans or corals; Pl. 6, Figs. 1-3; Pl. 7, Figs. 1, 2). The rocks are weakly burrowed (Pl. 6, Fig. 3; Pl. 7, Fig. 4; Pl. 8, Fig. 2) or sometimes perforated by various organisms. Bioclasts are dispersed or form interlayered thin laminae a few mm thick (Pl. 7, Fig. 3). Rare ferruginous microstromatolites and iron-encrusted shells (Pl. 7, Fig. 3-6; Pl. 8, Figs. 1, 3) are also present. The matrix is frequently clotted (Pl. 7, Fig. 2; Pl. 8, Fig. 4), and shows small filiform fenestrae suggesting alteration of sponges. These latter are locally abundant forming nodular bafflestones — the nodular texture being accentuated by pressure solution (Pl. 6, Fig. 4). Abundant small hematitized bacterial microtufts, blisters, and curved filaments are disseminated in the matrix of all microfacies (Pl. 6, Fig. 1; Pl. 7, Figs. 3-6; Pl. 8, Figs. 3-6). They also underline thin, discontinuous hardground levels. These ferruginous biostructures are similar to those described by MAMET *et al.* (1997) from the Lower Devonian of the

Czech Republic, or by PRÉAT *et al.* (1999) from the Frasnian-Famennian boundary GSSP of Coumiac, Montagne Noire. A few radiolarians are present in the facies above the dark grey Hangenberg Shale (sample 32, Fig. 2), and the boundary series is capped by meter thick cherty formations (lydites) rich in radiolarians (Pl. 6, Figs. 5, 6). Polished sections indicate that iron occurs as hematite and goethite, the latter surrounding the former displaying numerous small cracks. Rare pyrite (< 2 µm) occurs in the central part of ferruginized grains.

Despite the difficulty to reconstruct a bathymetric profile, the environment inferred is that of quiet and deeper waters, below or near the storm wave base, and without evidence of turbidite and mudflows. Sedimentation is assumed to have been below the photic zone as suggested by the absence of algae, and thin interlayered bioclastic laminae could represent tempestites *sensu* AIGNER (1985). The general depositional setting was probably that of a distal carbonate ramp, with an inferred depth around 100 m. Free oxygen was episodically low as suggested by the development near the seawater-sediment interface of iron-microbial(?) encrustations that are somewhat similar to those described from the Lower Devonian of the Czech Republic (MAMET *et al.*, 1997), or from the Devonian of the Montagne Noire (PRÉAT *et al.*, 1999). Dysaerobic conditions developed also in the sediment as indicated by the low degree of bioturbation and the scarcity of benthic macro- and microfauna, except for ostracods, particularly in the upper Famennian. Hematitized microtufts are probably the remains of min-

eral-microbial communities living at the seawater-sediment interface and accumulating ferric iron minerals comparable to those of the Devonian section at Coumiac, Montagne Noire (PRÉAT *et al.*, 1999).

Ostracods (J.-G. Casier & F. Lethiers)

Ostracod distribution and general remarks

Nineteen samples were collected across the Devonian-Carboniferous boundary in the Puech de la Suque section, covering the Middle *praesulcata* and the lower part of the *duplicata* conodont Zones (Fig. 2). More than 4,750 carapaces and relatively few valves of ostracods have been extracted by the hot acetolysis method (LETHIERS & CRASQUIN-SOLEAU, 1988). They are generally well preserved, except for sample PS6 from the upper part of the Hangenberg horizon.

Ostracods are abundant in samples PS1 and PS2, and extremely abundant in samples PS3 and PS4 of the Middle *praesulcata* Zone. They are absent in the lower (sample PS5) and scarce in the upper part (sample PS6) of the Hangenberg horizon. Above this unit, ostracods become relatively abundant again.

Thirteen ostracod species were already reported by LETHIERS & FEIST (1991) from the Famennian of the Puech de la Suque section. These species, included also in this account, were collected between the Hangenberg horizon and the Devonian-Carboniferous boundary (samples 7 and 8). In addition, 44 species were also reported (*Ibid.*) from the lower Tournaisian sequence and uppermost part of the “Griotte Limestone Formation” (*cooperi* conodont Zone) above the interval investigated and documented.

Ostracod systematics and listing of species identified

Order Palaeocopida HENNINGSMOEN, 1953
Suborder Palaeocopina HENNINGSMOEN, 1953

Superfamily Kirkbyacea ULRICH & BASSLER, 1906

Family Amphissitidae KNIGHT, 1928

- *Amphissites* sp. A (Pl. 1, Fig. 1, 2).

Superfamily Aparachitacea JONES, 1901

Family Rozhdestvenskayitidae MCGILL, 1966

- *Rozhdestvenskayites* cf. *pistrakae* (TSCHIGOVA, 1958) (Pl. 1, Fig. 3).

Superfamily Primitiopsacea SWARTZ, 1936

Family Graviidae POLENOVA, 1952

- *Coryellina* sp. A, aff. *grandis* ROBINSON, 1978 (Pl. 1, Fig. 4).

- *Coryellina* cf. *tenuisulcata* OLEMPSKA, 1979 (Pl. 1, Fig. 5).

Suborder Paraparchiticopina GRAMM
in GRAMM & IVANOV (1975)

Superfamily Paraparchitacea SCOTT, 1959

Family Paraparchitidae SCOTT, 1959

- *Proparaparchites?* *procerus* nov. sp. (Pl. 1, Fig. 6-9).

- *Paraparchites puechdelasuquensis* nov. sp. (Pl. 1, Fig. 10-13).

- *Shivaella* sp. indet. (Pl. 1, Fig. 14).

Order Podocopida SARS, 1866
Suborder Metacopina SYLVESTER-BRADLEY, 1961

Superfamily Thlipsuracea ULRICH, 1884

Family Quasillitidae CORYELL & MALKIN, 1936

- *Graphiadactylloides* sp. (Pl. 1, Fig. 15).

- *Ovatoquasillites slowikensis* (OLEMPSKA, 1981) (Pl. 2, Fig. 2).

Superfamily Healdiacea HARLTON, 1933

Family Healdiidae HARLTON, 1933

- *Timorhealdia nitidula nitidula* (RICHTER, 1869) (Pl. 1, Fig. 16).

- *Aurigerites obernitzensis* GRÜNDDEL, 1962 (Pl. 1, Fig. 17).

- *Aurigerites blumenstengeli* OLEMPSKA, 1979 (Pl. 2, Fig. 1).

- “*Aurigerites*” sp. A (Pl. 2, Fig. 3).

Suborder Podocopina SARS, 1866

Superfamily Cytheracea BAIRD, 1850

Family Bythocytheridae SARS, 1926

- *Bythoceratina* (P.) sp. GRÜNDDEL (1973)

Superfamily Bairdiocypridacea SHAVER, 1961

Family Bairdiocyprididae SHAVER, 1961

- *Healdianella lumbiformis* LETHIERS & FEIST, 1991 (Pl. 2, Fig. 4).

- *Healdianella* cf. *insolita* (BUSCHMINA, 1977) (Pl. 2, Fig. 5).

- *Praepilatina adamczaki* OLEMPSKA, 1979 (Pl. 2, Fig. 6).

- *Bairdiocypris* cf. *felix* ROZHDESTVENSKAJA, 1972 (Pl. 2, Fig. 8).

Family Pachydomellidae BERDAN & SOHN, 1961

- *Microneosomites elatus* (LETHIERS, 1978) (Pl. 2, Fig. 7).

- *Decoranewsomites blessi* (OLEMPSKA, 1979) (Pl. 2, Fig. 9).

- *Microcheilinella voronensis* SAMOLOVA, 1970 (Pl. 2, Fig. 10).

- *Microcheilinella* cf. *bushmina* OLEMPSKA, 1981 (Pl. 2, Fig. 11).

- “*Tubilibairdia*” gr. *unispina* BLUMENSTENGEL, 1965.

- *Grammia* cf. *aculeata* (BUSCHMINA, 1975) (Pl. 2, Fig. 12).

- *Grammia* nov. sp. A (Pl. 2, Fig. 13).

- *Rectoplacera* cf. *dorsocerata* BLUMENSTENGEL, 1979 sensu BECKER (1981).

- *Rectoplacera?* cf. sp. 1 OLEMPSKA, 1997 (Pl. 2, Fig. 14).

- *Triplacera triquetra* GRÜNDDEL, 1961.

Family Gerodiidae GRÜNDDEL, 1962

- *Baschkirina nandanensis* WANG, 1988 (Pl. 3, Fig. 1).

- *Gerodia weyeri olempskae* nov. subsp. (Pl. 3, Fig. 2, 3).

- *Gerodia?* sp. A BECKER, 1987 (Pl. 3, Fig. 4).

- *Paragerodia subtrapezoidalis* WANG, 1988.

- *Paragerodia?* sp. A (Pl. 3, Fig. 5).

Family Rectonariidae GRÜNDDEL, 1962

- *Orthonaria rectagona* (GRÜNDDEL, 1962) (Pl. 3, Fig. 7).

- *Orthonaria gruendeli* OLEMPSKA, 1979 (Pl. 3, Fig. 6).

- *Orthonaria neotridentifer* LETHIERS & FEIST, 1991 (Pl. 3, Fig. 9).
- *Rectonaria inclinata* GRÜNDDEL, 1961 (Pl. 3, Fig. 8).
- *Rectonaria kowalensis* OLEMPSKA, 1979 (Pl. 3, Fig. 12).
- *Rectonaria muelleri* GRÜNDDEL, 1961 (Pl. 3, Fig. 10).
- *Rectonaria varica* GRÜNDDEL, 1961 (Pl. 3, Fig. 11).

Superfamily Bairdiacea SARS, 1888

Family Acritidae GRÜNDDEL, 1962

- *Famenella angulata perparva* LETHIERS & FEIST, 1991 (Pl. 4, Fig. 1).
- *Acratia bidecliva* LETHIERS & FEIST, 1991 (Pl. 4, Fig. 2).
- *Acratia incurvata* LETHIERS & FEIST, 1991 (Pl. 4, Fig. 4).
- *Acratia sagittaeformis* LETHIERS & CASIER, 1999 subsp. (Pl. 4, Fig. 3).
- *Acratia cooperi* GRÜNDDEL, 1962 (Pl. 4, Fig. 6).
- *Acratia cf. insolita* BUSCHMINA, 1970 (Pl. 4, Fig. 5).
- *Acratia aff. rostrataformis* SCHEVTSOV, 1964 sensu BECKER (1982) (Pl. 4, Fig. 7).
- *Acratia nov. sp. A* (Pl. 4, Fig. 8).
- *Clinacratia clinata* (BLUMENSTENGEL, 1965) (Pl. 4, Fig. 9).
- *Ceratacratia cerata* BLUMENSTENGEL, 1965 (Pl. 4, Fig. 10).

Family Bairdiidae SARS, 1888

- *Bairdia (B.) feliumgibba* BECKER, 1982 (Pl. 4, Fig. 12).
- *Bairdia (B.) extenuata* NAZAROVA, 1951 (Pl. 4, Fig. 13).
- *Bairdia (B.) cf. galinaeformis* LETHIERS, 1981 (Pl. 4, Fig. 11).
- *Bairdia cf. altiformis* BUSCHMINA, 1984 sensu WANG (1988) (Pl. 4, Fig. 15).
- *Bairdia cf. subaryshtensis* BUSCHMINA, 1984 (Pl. 4, Fig. 14).
- *Bairdia (R.) superba* LETHIERS, 1981 subsp. A (Pl. 5, Fig. 1).
- *Bairdia (R.) nov. sp. A* (Pl. 5, Fig. 2).
- *Bairdia (R.) sp. aff. romei* LETHIERS, 1974.
- *Bairdia* sp. A BECKER, 1993 (Pl. 4, Fig. 16).
- "Bairdia" nov. sp. B CASIER & LETHIERS, 2000 (Pl. 5, Fig. 4).
- *Bohlenatia rhenothuria* BECKER, 1993 (Pl. 5, Fig. 3).
- *Processobairdia spinomarginata* BLUMENSTENGEL, 1965 (Pl. 5, Fig. 5).
- *Bairdiacypris virga* BUSCHMINA, 1970 (Pl. 5, Fig. 6).
- *Bairdiacypris* cf. *subcylindrica* BUSCHMINA, 1984 (Pl. 5, Fig. 8).
- *Bairdiacypris* cf. *quasielongata* BUSCHMINA, 1968 (Pl. 5, Fig. 7).
- *Parabairdiacypris? demigrans* BECKER, 1982? (Pl. 5, Fig. 9).

Order Myodocopida SARS, 1866
Suborder Myodocopina SARS, 1866

Superfamily Cypridinacea BAIRD, 1850

Family Cypridinidae BAIRD, 1850

- *Absina (A.) ventrorostrata* GRÜNDDEL, 1962.

Superfamily Entomozoacea PRIBYL, 1951

Family Entomozoidae PRIBYL, 1950

- *Richterina (R.) striatula* (RICHTER, 1848) (Pl. 5, Fig. 10).
- *Richterina (R.) tenuistriata* KUMMEROW, 1939?
- *Richterina (Fossirichterina) semen* (JONES, 1895) (Pl. 5, Fig. 11).
- *Richterina?* sp.
- *Maternella (M.) cf. empleura* (KUMMEROW, 1939) (Pl. 5, Fig. 12).

Description of two new species and one new subspecies

Types are deposited in the collections of the Department of Palaeontology (Section Micropalaeontology) of the Belgian Royal Institute of Natural Sciences (IRScNB n° b...).

Genus *Proparaparchites* COOPER, 1941

TYPE-SPECIES

Proparaparchites ovatus COOPER, 1941.

Proparaparchites? procerus nov. sp.

(Pl. 1, Fig. 6-9)

DERIVATIO NOMINIS

The name is derived from Latin *procerus* = long, referring to the elongation of the carapace.

TYPES

Holotype: Carapace. (Pl. 1, Fig. 6). PS3. IRScNB n° b3703. L = 0.53 mm; H = 0.19 mm; W = 0.21 mm.
Paratype A: Carapace. (Pl. 1, Fig. 7). PS2. IRScNB n° b3704. L = 0.43 mm; H = 0.16 mm; W = 0.18 mm.
Paratype B: Carapace. (Pl. 1, Fig. 8). PS4. IRScNB n° b3705. L = 0.49 mm; H = 0.21 mm; W = 0.21 mm.
Paratype C: Carapace. (Pl. 1, Fig. 9). PS3. IRScNB n° b3706. L = 0.41 mm; H = 0.16 mm; W = 0.18 mm.

LOCUS TYPICUS

Puech de la Suque section, Montagne Noire, France.

STRATUM TYPICUM

Upper Famennian, Middle *praesulcata* conodont Zone.

MATERIAL

13 carapaces.

DIAGNOSIS

A small, elongate ($L/H = 2.4$) species belonging probably to the genus *Proparaparchites* with dorsal and ventral borders parallel, and straight or gently arched. Ventral part of the carapace flattened with fine marginal bends.

DESCRIPTION

In lateral outline small, amplete, and elongate carapace. Dorsal and ventral borders parallel, straight or gently arched. Hinge line straight and slightly depressed. Anterior margin regularly curved but occasionally more curved antero-dorsally. Posterior margin more curved ventrally. Posterior cardinal angle strongly obtuse. Ventral part of the carapace sometimes flattened with marginal shoulders which are more developed on the right valve. Anterior extremity at half height or slightly

Table 1 — Distribution of ostracods close to the Devonian-Carboniferous boundary in the Puech de la Suque section. * = species belonging to the Thuringian ecotype; + = species belonging to the Myodocopid ecotype. Other species belong to the Eifelian ecotype. Column in grey = Hangenberg horizon.

above. Posterior extremity and maximum length at mid-height. Valves almost equal in size. In dorsal view, carapace regularly biconvex, except for the posterior part of the right valve which is occasionally compressed. Surface of valves smooth.

REMARKS

Proparaparchites? *procerus* nov. sp. differs from *P. ovatus* COOPER, 1941, *P. fabulus* COOPER, 1941, and *P. parallelus* COOPER, 1946 — all from the Carboniferous of Illinois —, and from *P. tersiensis* BUSCHMINA, 1968 from the Upper Tournaisian of the Kuznetsk Basin by its elongation, by the flattening of the ventral part of the carapace, and by the presence of marginal shoulders. This last character is unusual, and the generic placement therefore uncertain.

OCCURRENCE

Upper Famennian of the Puech de la Suque section (samples PS2-4).

Genus *Paraparchites* ULRICH & BASSLER, 1906,
emend. SOHN, 1971

TYPE-SPECIES

Paraparchites humerosus ULRICH & BASSLER, 1906.

***Paraparchites puechdelasquensis* nov. sp.**
(Pl. 1, Fig. 10-13)

1997 *Shemonella* sp. - OLEMPSKA, p. 326, fig. 7d-f.

DERIVATIO NOMINIS

From the Puech de la Suque hill, in the Montagne Noire, France.

TYPES

Holotype: Carapace. (Pl. 1, Fig. 10). PS3. IRSNB n° b3707. L = 0.57 mm; H = 0.38 mm; W = 0.28 mm.
Paratype A: Carapace. (Pl. 1, Fig. 11). PS2. IRSNB n° b3708. L = 0.62 mm; H = 0.41 mm; W = 0.35 mm.
Paratype B: Carapace. (Pl. 1, Fig. 12). PS4. IRSNB n° b3709. L = 0.50 mm; H = 0.31 mm; W = 0.23 mm.
Paratype C: Carapace. (Pl. 1, Fig. 13). PS3. IRSNB n° b3710. L = 0.52 mm; H = 0.38 mm; W = 0.27 mm.

LOCUS TYPICUS

Puech de la Suque section, Montagne Noire, France.

STRATUM TYPICUM

Upper Famennian, Middle *praesulcata* conodont Zone.

MATERIAL

19 carapaces and valves.

DIAGNOSIS

A small, preplete species of *Paraparchites* with a very short, nearly straight dorsal border. Hinge line slightly depressed, and maximum width at mid-length.

DESCRIPTION

A small, preplete and elliptical carapace in lateral out-

line. Dorsal border straight or gently arched. Ventral border more curved anteriorly. Anterior and posterior borders broadly rounded. Anterior extremity at mid-height. Posterior extremity between half and dorsal third of eight. Hinge line short, straight, and slightly depressed. Left valve overlapping the right all along the free border but no dorsal overreach. In dorsal view, carapace regularly biconvex. Maximum width at mid-length. Dimorphism unknown. Surface of valves smooth.

REMARKS

The probably polyphyletic (SOHN, 1971) genus *Paraparchites* is represented by numerous species in the Lower Carboniferous. In contrast, few species have been recognized in the Upper Devonian. Among them is *Paraparchites* sp. BLUMENSTENGEL, 1995 from do VI of Thuringia (Germany) which is greater and more elongate than *P. puechdelasquensis* nov. sp. The outline of *Shemonella* sp. figured by OLEMPSKA (1997) of the Kowala section of Poland, and its seemingly short, straight, and slightly depressed hinge are features similar to those observed in *P. puechdelasquensis* nov. sp. The small size of the carapaces and the other diagnostic characters are sufficient to differentiate the new species from Carboniferous and Permian species.

OCCURRENCE

Upper Famennian beds of the Puech de la Suque section (samples PS1-4). Probably also upper Famennian of the Kowala section of Poland (OLEMPSKA, 1997).

Genus *Gerodia* GRÜNDDEL, 1962

TYPE-SPECIES

Gerodia ratina GRÜNDDEL, 1962.

Gerodia weyeri GRÜNDDEL, 1972

DIAGNOSIS (after GRÜNDDEL, 1972)

A species belonging to the genus *Gerodia* with a subtrapezoidal outline, a distinctly inflated carapace, a marginal ridge on the postero- and antero-ventral borders of the right valve, and a more or less developed postero-ventral spine on the right valve.

***Gerodia weyeri weyeri* GRÜNDDEL, 1972**

*	1972	<i>Gerodia weyeri</i> GRÜNDDEL - GRÜNDDEL, p. 860-861, fig. 2.
v.	1986	<i>Gerodia weyeri</i> GRÜNDDEL, 1972 - DELVOLVÉ & LETHIERS, p. 495, Pl. 1, Fig. 10.
.	1999	<i>Gerodia weyeri</i> GRÜNDDEL 1972 - BECKER, p. 63, pl. 7, Fig. 13-15.
?	1999	<i>Gerodia</i> sp., Gruppe <i>weyeri</i> GRÜNDDEL 1972 - BECKER, p. 63, pl. 17, Fig. 8-9.

DIAGNOSIS

As for *Gerodia weyeri* GRÜNDDEL, 1972.

OCCURRENCE

Late Famennian (doVI) of Germany and France (Western Pyrénées).

***Gerodia weyeri olempskae* nov. subsp.**
(Pl. 3, Fig. 2, 3)

- . 1979 *Gerodia weyeri* GRÜNDEL, 1972 - OLEMPSKA, p. 123, pl. 25, Fig. 8, 9.
- . 1981 *Gerodia weyeri* GRÜNDEL - OLEMPSKA, tabl. 1, 2.

DERIVATIO NOMINIS

In honour of Dr. Ewa Olempska, Polish Academy of Sciences.

TYPES

Holotype: Carapace. (Pl. 3, Fig. 3). PS4. IRSNB n° b3731. L = 0.61 mm; H = 0.38 mm; W = 0.41 mm.

Paratype A: Carapace of a poorly preserved adult. (Pl. 3, Fig. 2). PS4. IRSNB n° b3730. L = 1.36 mm; H = 0.77 mm; W = 0.92 mm.

Paratype B: Carapace. PS16. IRSNB n° b3732. L = 0.50 mm; H = 0.30 mm; W = 0.30 mm.

LOCUS TYPICUS

Puech de la Suque section, Montagne Noire, France.

STRATUM TYPICUM

Upper Famennian, Middle *praesulcata* conodont Zone.

MATERIAL

27 carapaces and valves.

DIAGNOSIS

A subspecies of *Gerodia weyeri* GRÜNDEL, 1972, without well-defined postero-ventral spine.

DESCRIPTION

In lateral outline, large, amplete or slightly post-plete elliptical carapace. Dorsal and ventral borders moderately and regularly arched. Anterior border regularly curved, and posterior border more curved in the postero-ventral sector. Anterior extremity at mid-height. Posterior extremity between the half and the ventral third of height. Hinge line short, straight and slightly depressed. Ventral surface of carapace somewhat flattened. Left valve overreaching the right one all along the free border and particularly ventrally. Delicate marginal ridge on the postero- and antero-ventral borders of the right valve. In dorsal view, carapace strongly biconvex. Carapace slightly wider than high, and maximum width at mid-length. No well-defined postero-ventral spine. Surface of valves smooth.

REMARKS

Previously, OLEMPSKA (1979) suggested that the specimens of *Gerodia weyeri* which she found in the upper Famennian of the Kowala section of Poland should be assigned to a new subspecies, the subspecies proposed.

OCCURRENCE

Upper Famennian and lower Tournaisian strata of the Puech de la Suque section (samples PS1, 3, 4, 9, 10, 13, 16, 18?). Upper Famennian of the Kowala and Jablonna sections in Poland (OLEMPSKA, 1997).

Ostracods and the Hangenberg Event

The study of ostracods from Thuringia (Germany) by BLUMENSTENGEL (1993) has revealed the disappearance of many ostracod species as a result of the Hangenberg Event. Only 18 species out of 53 belonging to the Thuringian ecotype (indicative of calm, deeper and/or cold marine environments) and Myodocopid ecotypes (indicative of calm, dysoxic environments) were reported to have survived the event in that region. In contrast, WALLISER (1984) and GROOS-UFFENORDE & SCHINDLER (1990) came to the conclusion that no major change took place during the Hangenberg Event for the Entomozoacea (Myodocopida), and BECKER & BLUMENSTENGEL (1995) surmised that only ubiquitous ostracods of the Thuringian ecotype survived the event.

From the Holy Cross Mountains of Poland, OLEMPSKA (1997) reported a major change in ostracods belonging both to the Thuringian and Myodocopid ecotypes close to the Devonian - Carboniferous boundary. Only 14 species out of 37 belonging to the Thuringian ecotype present in the upper Famennian of the Kowala section, occur also in the lower Carboniferous, and all Entomozoacea (Myodocopida) species were replaced. Nevertheless, OLEMPSKA concluded that the Kowala faunal changes were strictly local biotic events (*Ibid.*, p.308).

Ostracods of the Hangenberg horizon and across the Devonian - Carboniferous boundary in the Puech de la Suque section

Seventy-two ostracod species have so far been identified in the Puech de la Suque section (Tab. 1), half of which belongs to the Thuringian ecotype. Below the Hangenberg horizon, ostracods representing the Myodocopid ecotype are relatively frequent but belong to three species only: *Richterina (R.) striatula* (RICHTER, 1848), *Richterina (Fossirichterina) semen* (JONES, 1895), and *Richterina?* sp. Three Entomozoacea — one *Richterina?* sp. and probably two *Richterina (R.) teuistriata* KUMMEROW, 1939 — were recovered from the Late *praesulcata* and *sulcata* conodont Zones straddling the Devonian - Carboniferous boundary. In the lower part of the Tournaisian *duplicata* Zone, myodocopid ostracods once again are relatively frequent but represented by only one species: *Maternella (M.) cf. empleura* (KUMMEROW, 1939). Between the Hangenberg horizon and the Devonian - Carboniferous boundary, ostracods of the Thuringian ecotype become relatively more abundant than ostracods belonging to the Eifelian ecotype reflecting possibly an increase in sea level as suggested by the presence of radiolarians in thin sections.

Only 16 (or at the maximum 18) species out of 48 present below the Hangenberg horizon disappeared in the Puech de la Suque section. However our Famennian species *Coryellina grandis* ROBINSON, 1978 *sensu* OLEMPSKA (1997) is known also from the Tournaisian of Poland, *Parabairdiacypris? demigrans* BECKER, 1982 from the Carboniferous of the Sauerland of Germany (BECKER *et al.*, 1993), and *Richterina (R.) striatula* (RICHTER, 1898) from the Carboniferous of Thuringia

(Germany) and Poland (RABIEN, 1960; BLASZYK & NATUSIEWICZ, 1973). In addition, *Clinacratia clinata* (BLUMENSTENGEL, 1965) should be present according to BECKER (1987) in the Carboniferous of the Harz Mountains of Germany and of the Algerian Sahara region. In general, a total of 12 to 15 species recovered from the upper Famennian strata disappeared as a result of the Hangenberg Event, and hence the rate of extinction is between 25 and 31.5 percent. Of course, no disappearance of ostracods is recorded at the Devonian - Carboniferous boundary.

Furthermore, there is also a notable qualitative difference among the disappearing ostracod species: only 17 percent of the Thuringian ecotype ostracods are involved whereas half of the Eifelian ecotype ostracods did not survive the Hangenberg Event.

Conclusions

The rate of extinction of ostracod species associated with the Hangenberg Event is low in the Puech de la Suque section in comparison with the rate observed during the worldwide Frasnian - Famennian changeover (see: LETHIERS & CASIER, 1999 and CASIER & LETHIERS, 2001 for more information about the ostracods and this last event). A maximum of 31.5 percent of species disappeared as a result of the Hangenberg Event in comparison the 75 percent worldwide at the Frasnian - Famennian boundary, and there are no "disaster species" associated

with the Hangenberg Event as there are in the Frasnian - Famennian crisis.

No significant paleo-environmental changes seemingly occurred at the Devonian - Carboniferous boundary or within the Hangenberg Shale in the section studied, except that this level contains reddish-coloured thin carbonate beds suggesting temporarily more pronounced dysaerobic conditions in the sediment, as interpreted by PRÉAT *et al.* (1999). The presence of radiolarians above this shale could indicate that an increase in sea level, takes place in the Puech de la Suque section above the Hangenberg Horizon. The presence of various discontinuous hardgrounds furthermore suggest that the rate of sedimentation has frequently changed.

The increase of the relative abundance of ostracods belonging to the Thuringian ecotype above the Hangenberg horizon possibly reflects the rise in sea level as deduced also from the sedimentological evidence and facies analysis. However, the Thuringian-type ostracods are also known to be more resistant to dysaerobic water conditions (LETHIERS & FEIST, 1991).

Acknowledgments

We wish to thank Dr. Ewa Olempska of the Polish Academia of Sciences and especially Professor Emeritus Willi K. Braun of Saskatchewan University, for their detailed review of our manuscript and for many useful suggestions. This work has been supported by the C.N.R.S. ESA 7073 and Crisevole Programs.

References

- AIGNER, T., 1985. Storm depositional systems. Springer Verlag, Berlin, 174 p.
- BECKER, G., 1987. Ostracoda des Thüringer Ökotyps aus dem Grenzbereich Devon/Karbon N-Afrikas (Marokko, Algerien). *Palaeontographica*, A, **200**: 45-104.
- BECKER, G., 1999. Verkieselte Ostracoden vom Thüringer Ökotyp aus den Devon/Karbon-Grenzschichten (Top Wocklumer Kalk und Basis Hangenberg-Kalk) im Steinbruch Dreher (Rheinisches Schiefergebirge). *Courier Forschungsinstitut Senckenberg*, **218**, 159 p.
- BECKER, G. & BLUMENSTENGEL, H., 1995. The importance of the Hangenberg event on ostracod distribution at the Devonian-Carboniferous boundary in the Thuringian and Rhenish Schiefergebirge. In: RIHA, J. ed. Ostracoda and Biostratigraphy. Balkema, Rotterdam, Brookfield: 67-78.
- BECKER, G., CLAUSEN, C.-D. & LEUTERITZ, K., 1993. Verkieselte Ostracoden vom Thüringer Ökotyp aus dem Grenzbereich Devon/Karbon des Steinbruchs Dreher (Rheinisches Schiefergebirge). *Courier Forschungsinstitut Senckenberg*, **160**: 1-139.
- BECKER, R. T., 1993. Anoxia, eustatic changes, and Upper Devonian to Lowermost Carboniferous global ammonoid diversity. *The Systematics Association*, sp. vol. **47**: 115-164.
- BLASZYK, J. & NATUSIEWICZ, D., 1973. Carboniferous ostracods from the borings in north-western Poland. *Acta Palaeontologica Polonica*, **18**, 1: 117-151.
- BLUMENSTENGEL, H., 1993. Ostracodes from the Devonian-Carboniferous boundary beds in Thuringia (Germany). *Annales de la Société géologique de Belgique*, **115** (1992), 2: 483-489.
- BOYER, F., KRYOLATOV, S., LE FEVRE, J. & STOPPEL, O., 1968. Le Dévonien supérieur et la limite dévono-carbonifère en Montagne Noire (France). Lithostratigraphie-biostratigraphie (conodontes). *Bulletin des Centres de Recherche Exploration-Production Elf-Aquitaine*, 2: 5-33.
- CAPLAN, M. & BUSTIN, R., 1999. Devonian-Carboniferous Hangenberg mass extinction event, widespread organic-rich mudrock and anoxia: causes and consequences. *Palaeogeography, Palaeoclimatology, Palaeoecology*, **148**: 187-207.
- CASIER, J.-G. & LETHIERS, F., 2001. Ostracods prove that the F/F boundary mass extinction was a major and abrupt crisis. *Lecture Notes in Earth Sciences* (in print).
- COOPER, C., 1941. Chester Ostracodes of Illinois. *Report of investigations of the Illinois State Geological Survey*, **77**, 101 p.
- COOPER, C., 1946. Pennsylvanian Ostracodes of Illinois. *Bulletin of the Illinois State Geological Survey*, **70**: 1-177.
- COPPER, P., 1998. Evaluating the Frasnian-Famennian mass extinction: comparing brachiopod faunas. *Acta Palaeontologica Polonica*, **43**, 2: 137-154.
- DELVOLVÉ, J.-J. & LETHIERS, F. 1986. Découverte d'une remarquable faune profonde d'ostracodes d'âge strunien, près d'Hendaye (Pyrénées occidentales). *Comptes rendus de l'Académie des Sciences*, Paris, **302**, Série II: 491-496.
- FEIST, R., 1995. Devonian Stratigraphy of the southeastern Montagne Noire (France). *Courier Forschungsinstitut Senckenberg*, **75**: 331-352.
- FEIST, R. ed., 1990. The Frasnian-Famennian boundary and adjacent strata of the Eastern Montagne Noire, France. *Guide book of the Field Meeting, Montagne Noire 1990, International*

- Union of Geological Sciences, Subcommission Devonian Stratigraphy, Montpellier: 1-69.
- FEIST, R., 1991. The Late Devonian trilobite crisis. *Historical Biology*, **5**: 197-214.
- FEIST, R. & FLAJS, G., 1987. La limite Dévonien-Carbonifère dans la Montagne Noire (France). Biostratigraphie et environnement. *Comptes rendus de l'Académie des Sciences, Paris*, **305**, Série II: 1537-1544.
- FLAJS, G. & FEIST, R., 1988. Index conodonts, trilobites and environment of the Devonian-Carboniferous boundary at La Serre (Montagne Noire, France). *Courier Forschungsinstitut Senckenberg*, **100**: 53-107.
- GIRARD, C., 1996. Réponse des communautés de conodontes aux perturbations eustatiques: les événements fini-dévoniens dans la Montagne Noire (France). *Revue de Micropaléontologie*, **39**, 4: 261-270.
- GROOS-UFFENORDE, H. & SCHINDLER, E., 1990. The effect of global events on entomozoacean Ostracoda. In: WHATLEY, R. & MAYBURY, C. eds. Ostracoda and Global Events. *British Micropalaeontological Society Publication Series*, Chapman & Hall: 101-112.
- GRÜNDL, J., 1972. Eine neue Ostracodenart aus der Wocklumeria-Stufe (Oberdevon). *Geologie*, **21** (7): 859-861.
- GRÜNDL, J., 1973. Bythocytheridae (Ostracoda) aus dem Oberdevon/Dinant des Thüringer Schiefergebirges. *Zeitschrift fuer geologische Wissenschaften*, **1** (3): 329-345.
- HALLAM, A. & WIGNALL, P., 1997. Mass extinctions and their aftermath. Oxford University Press, 320 p.
- HOUSE, M., 1985. Correlation of mid-Palaeozoic ammonoid evolutionary events with global sedimentary perturbations. *Nature*, **313**: 17-22.
- HOUSE, M., 1993. Fluctuations in ammonoid evolution and possible environmental controls. *The Systematics Association*, sp. vol. **47**: 13-34.
- LETHIERS, F. & CASIER, J.-G., 1999. Autopsie d'une extinction biologique. Un exemple: la crise de la limite Frasnian - Famennian (384 Ma). *Comptes rendus de l'Académie des Sciences, Paris, Earth & Planetary Sciences*, **329**: 303-315.
- LETHIERS, F. & CRASQUIN-SOLEAU, S., 1988. Comment extraire les microfossiles à tests calcitiques des roches calcaires dures. *Revue de Micropaléontologie*, **31**, 1: 56-61.
- LETHIERS, F. & FEIST, R., 1991. Ostracodes, stratigraphie et bathymétrie du passage Dévonien-Carbonifère au Viséen Inférieur en Montagne Noire (France). *Geobios*, **24**, 1: 71-104.
- MAMET, B., PRÉAT, A. & DE RIDDER, C., 1997. Bacterial origin of the red pigmentation in the Devonian Slivenec Limestone, Czech Republic. *Facies*, **36**: 173-188.
- MICHEL, D., 1981. Paléoenvironnement des calcaires noduleux et lydiennes en Montagne Noire (Dévonien sup.-Dinantien); Sédimentologie, approche expérimentale et géochimie. *Thèse 3e cycle*, Paris Sud, 385 p. (inédit).
- OLEMPSKA, E., 1979. Middle to Upper Devonian Ostracoda from the southern Holy Cross Mountains, Poland. *Palaeontologia Polonica*, **40**: 57-162.
- OLEMPSKA, E., 1981. Lower Carboniferous ostracodes of the Holy Cross Mountains, Poland. *Acta Palaeontologica Polonica*, **26**, 1: 35-53.
- OLEMPSKA, E., 1997. Changes in benthic ostracod assemblages across the Devonian-Carboniferous boundary in the Holy Cross Mountains, Poland. *Acta Palaeontologica Polonica*, **42**, 2: 291-332.
- PRÉAT, A., MAMET, B., BERNARD, A. & GILLAN, D., 1999. Bacterial mediation, red matrices diagenesis, Devonian, Montagne Noire (southern France). *Sedimentary Geology*, **126**: 223-242.
- RABIEN, A., 1960. Zur Ostracoden-Stratigraphie an der Devon-Karbon-Grenze im Rheinischen Schiefergebirge. *Fortschritte in der Geologie von Rheinland und Westfalen*, **3**, 1: 61-106.
- SCHMIDT, H., 1924. Zwei Cephalopodenfaunen an der Devon-Karbon-Grenze im Sauerland. *Jahrbuch der Preussischen geologischen Landesanstalt*, **44**: 98-171.
- SOHN, I., 1971. New late Mississippian ostracode genera and species from northern Alaska. *US Geological Survey Professional Paper*, **711-A**, 24 p.
- WALLISER, O., 1984. Pleading for a natural D/C boundary. *Courier Forschungsinstitut Senckenberg*, **67**: 241-246.
- WALLISER, O., 1996. Global events in the Devonian and Carboniferous. In: WALLISER, O. ed. Global events and event stratigraphy in the Phanerozoic. Springer, Berlin: 225-250.
- Jean-Georges CASIER
Département de Paléontologie
Section de Micropaléontologie-
Paléobotanique
Institut royal des Sciences naturelles de
Belgique
rue Vautier, 29, B-1000 Bruxelles,
Belgique
E-mail: casier@kbnirsnb.be
- Francis LETHIERS
Université Paris VI
Département de Géologie sédimentaire
Laboratoire de Micropaléontologie
4, place Jussieu, F-75252 Paris Cedex 05,
France
E-mail: lethiers@ccr.jussieu.fr
- Alain PRÉAT
Département des Sciences de la Terre et
de l'Environnement
Université libre de Bruxelles
Av. F.D. Roosevelt, 50, B-1050
Bruxelles,
Belgique
E-mail: apreat@ulb.ac.be
- Typescript submitted: 20.6.2000
Revised typescript received: 15.10.2000

PLATE 1

- Fig. 1 — *Amphissites* sp. A. Carapace. PS4. IRSNB n° b3698. x50. 1a: right lateral view; 1b: dorsal view.
- Fig. 2 — *Amphissites* sp. A. Broken carapace in right lateral view. PS3. IRSNB n° b3699. x100.
- Fig. 3 — *Rozhdestvenskayites* cf. *pistrakae* (TSCHIGOVA, 1958). Carapace. PS2. IRSNB n° b3700. x60. 3a: left lateral view; 3b: dorsal view.
- Fig. 4 — *Coryellina* sp. A, aff. *grandis* ROBINSON, 1978. Carapace. PS3. IRSNB n° b3701. x100. 4a: left lateral view; 4b: dorsal view.
- Fig. 5 — *Coryellina* cf. *tenuisulcata* OLEMPSKA, 1979. Carapace. PS3. IRSNB n° b3702. x60. 5a: right lateral view; 5b: dorsal view.
- Fig. 6 — *Proparaparchites?* *procerus* nov. sp. Holotype. PS3. IRSNB n° b3703. x80. 6a: right lateral view; 6b: dorsal view.
- Fig. 7 — *P.?* *procerus* nov. sp. Right lateral view of Paratype A. PS4. IRSNB n° b3704. x80.
- Fig. 8 — *P.?* *procerus* nov. sp. Paratype B. PS4. IRSNB n° b3705. x80. 8a: right lateral view; 8b: ventral view.
- Fig. 9 — *P.?* *procerus* nov. sp. Right lateral view of Paratype C. PS3. IRSNB n° b3706. x100.
- Fig. 10 — *Paraparchites puechdelasuquensis* nov. sp. Holotype. PS3. IRSNB n° b3707. x80. 10a: right lateral view; 10b: dorsal view.
- Fig. 11 — *P. puechdelasuquensis* nov. sp. Right lateral view of Paratype A. PS4. IRSNB n° b3708. x80.
- Fig. 12 — *P. puechdelasuquensis* nov. sp. Right lateral view of Paratype B. PS2. IRSNB n° b3709. x80.
- Fig. 13 — *P. puechdelasuquensis* nov. sp. Right lateral view of Paratype C. PS3. IRSNB n° b3710. x80.
- Fig. 14 — *Shivaella* sp. indet. Right valve. PS4. IRSNB n° b3711. x80.
- Fig. 15 — *Graphiadactylloides* sp. Carapace. PS19. IRSNB n° b3712. x60. 15a: right lateral view; 15b: dorsal view.
- Fig. 16 — *Timorhealdia nitidula nitidula* (RICHTER, 1869). Carapace. PS17. IRSNB n° b3713. x85. 16a: right lateral view; 16b: dorsal view.
- Fig. 17 — *Aurigerites obernitzensis* GRÜNDEL, 1962. Carapace. PS3. IRSNB n° b3714. x80. 18a: right lateral view; 18b: dorsal view.

PLATE 2

- Fig. 1 — *Aurigerites blumenstengeli* OLEMPSKA, 1979. Carapace. PS3. IRSNB n° b3715. x80. 1a: right lateral view; 1b: dorsal view.
- Fig. 2 — *Ovatoquasillites slowikensis* (OLEMPSKA, 1981). Right lateral view of a broken carapace. PS18. IRSNB n° b3716. x80.
- Fig. 3 — "Aurigerites" sp. A. PS13. Carapace. IRSNB n° b3717. x80. 3a: right lateral view; 3b: dorsal view.
- Fig. 4 — *Healdianella lumbiformis* LETHIERS & FEIST, 1991. Carapace. PS13. IRSNB n° b3718. x85. 4a: left lateral view; 4b: dorsal view.
- Fig. 5 — *Healdianella* cf. *insolita* (BUSCHMINA, 1977). Carapace. PS4. IRSNB n° b3719. x100. 5a: right lateral view; 5b: dorsal view.
- Fig. 6 — *Praepilatina adamczaki* OLEMPSKA, 1979. Carapace. PS1. IRSNB n° b3720. x100. 6a: left lateral view; 6b: dorsal view.
- Fig. 7 — *Micronewsomites elatus* (LETHIERS, 1978). Carapace. PS1. IRSNB n° b3721. x80. 7a: right lateral view; 7b: dorsal view.
- Fig. 8 — *Bairdiocypris* cf. *felix* ROZHDESTVENSKAJA, 1972. Carapace. PS3. IRSNB n° b3722. x80. 8a: right lateral view; 8b: dorsal view.
- Fig. 9 — *Decoranewsomites blessi* (OLEMPSKA, 1979). Carapace. PS3. IRSNB n° b3723. x80. 9a: right lateral view; 9b: dorsal view.
- Fig. 10 — *Microcheilinella voronensis* SAMOIOLOVA, 1970. Carapace. PS3. IRSNB n° b3724. x80. 10a: right lateral view; 10b: dorsal view.
- Fig. 11 — *Microcheilinella* cf. *bushminae* OLEMPSKA, 1981. Carapace. PS9. IRSNB n° b3725. x80. 11a: right lateral view; 11b: dorsal view.
- Fig. 12 — *Grammia* cf. *aculeata* (BUSCHMINA, 1975). Carapace. PS2. IRSNB n° b3726. 12a: right lateral view. x80; 12b: dorsal view. x85.
- Fig. 13 — *Grammia* nov. sp. A. Carapace. PS4. IRSNB n° b3727. x100. 13a: right lateral view; 13b: dorsal view.
- Fig. 14 — *Rectoplacera?* cf. sp. 1 OLEMPSKA, 1997. Right valve. PS9. IRSNB n° b3728. x80.

PLATE 3

- Fig. 1 — *Baschkirina nandanensis* WANG, 1988. Carapace. PS9. IRSNB n° b3729. x60. 1a: right lateral view; 1b: dorsal view.
- Fig. 2 — *Gerodia weyeri olempskae* nov. subsp. Right lateral view of Paratype A. PS4. IRSNB n° b3730. x50.
- Fig. 3 — *G. weyeri olempskae* nov. subsp. Holotype. PS4. IRSNB n° b3731. x80. 3a: right lateral view; 3b: dorsal view.
- Fig. 4 — *Gerodia?* sp. A BECKER, 1987. Carapace. PS4. IRSNB n° b3733. x60. 4a: right lateral view; 4b: dorsal view.
- Fig. 5 — *Paragerodia?* sp. A. Carapace. PS9. IRSNB n° b3734. x60. 5a: right lateral view; 5b: dorsal view.
- Fig. 6 — *Orthonaria gruendeli* OLEMPSKA, 1979. Carapace. PS4. IRSNB n° b3735. x100. 6a: right lateral view; 6b: dorsal view.
- Fig. 7 — *Orthonaria rectagona* (GRÜNDEL, 1962). Carapace. PS9. IRSNB n° b3736. x85. 7a: right lateral view; 7b: dorsal view.

- Fig. 8 — *Rectonaria inclinata* GRÜNDEL, 1961. Carapace. PS10. IRSNB n° b3737. x80. 8a: right lateral view; 8b: dorsal view.
- Fig. 9 — *Orthonaria neotridentifer* LETHIERS & FEIST, 1991. Carapace. PS13. IRSNB n° b3738. x100. 9a: right lateral view; 9b: dorsal view.
- Fig. 10 — *Rectonaria muelleri* GRÜNDEL, 1961. Carapace. PS13. IRSNB n° b3739. x70. 10a: left lateral view; 10b: dorsal view.
- Fig. 11 — *Rectonaria varica* GRÜNDEL, 1961. Carapace. PS13. IRSNB n° b3740. x100. 11a: right lateral view; 11b: dorsal view.
- Fig. 12 — *Rectonaria kowaleensis* OLEMPSKA, 1979. Carapace. PS4. IRSNB n° b3741. x75. 12a: right lateral view; 12b: dorsal view.

PLATE 4

- Fig. 1 — *Famenella angulata perparva* LETHIERS & FEIST, 1991. Carapace. PS15. IRSNB n° b3742. x80. 1a: right lateral view; 1b: dorsal view.
- Fig. 2 — *Acratia bidecliva* LETHIERS & FEIST, 1991. Right lateral view of a poorly preserved carapace. PS10. IRSNB n° b3743. x80.
- Fig. 3 — *Acratia sagittaeformis* LETHIERS & CASIER, 1999 subsp. Carapace. PS9. IRSNB n° b3744. x70. 3a: right lateral view; 3b: dorsal view.
- Fig. 4 — *Acratia incurvata* LETHIERS & FEIST, 1991. Left lateral view of a carapace. PS17. IRSNB n° b3745. x80.
- Fig. 5 — *Acratia cf. insolita* BUSCHMINA, 1970. Carapace. PS16. IRSNB n° b3746. x80. 5a: right lateral view; 5b: dorsal view.
- Fig. 6 — *Acratia cooperi* GRÜNDEL, 1962. Carapace. PS17. IRSNB n° b3747. x70. 6a: right lateral view; 6b: dorsal view.
- Fig. 7 — *Acratia aff. rostrataformis* SCHEVTSOV, 1964 sensu BECKER (1982). Carapace. PS2. IRSNB n° b3748. x80. 7a: right lateral view; 7b: dorsal view.
- Fig. 8 — *Acratia nov. sp. A.* Carapace. PS9. IRSNB n° b3749. x80. 8a: right lateral view; 8b: dorsal view.
- Fig. 9 — *Clinacratia clinata* (BLUMENSTENGEL, 1965). Carapace. PS1. IRSNB n° b3750. x80. 9a: right lateral view; 9b: ventral view.
- Fig. 10 — *Ceratacratia cerata* BLUMENSTENGEL, 1965. Carapace. PS3. IRSNB n° b3751. x80. 10a: right lateral view; 10b: dorsal view.
- Fig. 11 — *Bairdia (B.) cf. galinaeformis* LETHIERS, 1981. Right lateral view of a carapace. PS15. IRSNB n° b3752. x80.
- Fig. 12 — *Bairdia (B.) felumgibba* BECKER, 1982. Carapace. PS15. IRSNB n° b3753. x70. 12a: right lateral view; 12b: dorsal view.
- Fig. 13 — *Bairdia (B.) extenuata* NAZAROVA, 1951. Carapace. PS15. IRSNB n° b3754. x80. 13a: right lateral view; 13b: dorsal view.
- Fig. 14 — *Bairdia cf. subartyshensis* BUSCHMINA, 1984. Carapace. PS2. IRSNB n° b3755. x80. 14a: right lateral view; 14b: dorsal view.
- Fig. 15 — *Bairdia cf. altiformis* BUSCHMINA, 1984 sensu WANG (1988). Carapace. PS2. IRSNB n° b3756. x60. 15a: right lateral view; 15b: dorsal view.
- Fig. 16 — *Bairdia* sp. A BECKER 1993. Carapace. PS17. IRSNB n° b3757. x80. 16a: right lateral view; 16b: dorsal view.

PLATE 5

- Fig. 1 — *Bairdia (R.) superba* LETHIERS, 1981 subsp. A. Carapace. PS13. IRSNB n° b3758. x60. 1a: right lateral view; 1b: dorsal view.
- Fig. 2 — *Bairdia (R.) nov. sp. A.* Carapace. PS19. IRSNB n° b3759. x90. 2a: right lateral view; 2b: dorsal view.
- Fig. 3 — *Bohlenatia rhenothuria* BECKER, 1993. Carapace. PS4. IRSNB n° b3760. x50. 3a: right lateral view; 3b: dorsal view.
- Fig. 4 — "Bairdia" nov. sp. B CASIER & LETHIERS, 2000. Carapace. PS1. IRSNB n° b3761. x110. 4a: left lateral view; 4b: dorsal view.
- Fig. 5 — *Processobairdia spinomarginata* BLUMENSTENGEL, 1965. Carapace. PS3. IRSNB n° b3762. x80. 5a: right lateral view; 5b: dorsal view.
- Fig. 6 — *Bairdiacypris virga* BUSCHMINA, 1970. PS2. IRSNB n° b3763. x60. 6a: right lateral view; 6b: dorsal view.
- Fig. 7 — *Bairdiacypris cf. quasielongata* BUSCHMINA, 1968. Carapace. PS13. IRSNB n° b3764. x80. 7a: right lateral view; 7b: dorsal view.
- Fig. 8 — *Bairdiacypris cf. subcylindrica* BUSCHMINA, 1984. Carapace. PS15. IRSNB n° b3765. x70. 8a: right lateral view; 8b: dorsal view.
- Fig. 9 — *Parabairdiacypris? demigrans* BECKER, 1982? Carapace. PS2. IRSNB n° b3766. x70. 9a: right lateral view; 9b: dorsal view.
- Fig. 10 — *Richterina (R.) striatula* (RICHTER, 1848). Left valve. PS4. IRSNB n° b3767. x70.
- Fig. 11 — *Richterina (Fossirichterina) semen* (JONES, 1895). Carapace. PS3. IRSNB n° b3768. x100. 11a: right lateral view; 11b: dorsal view. The muscle scar is poorly developed on this specimen. Such intraspecific variation is common within the entomozooid ostracods. For instance, according to the development of the muscle scar, the species *costata* RICHTER, 1869 is sometimes assigned to the sub-genus *Richterina* GÜRICH, 1896 and sometimes to the sub-genus *Fossirichterina* MATERN, 1929. For the same reason, some Entomozoacea have probably been described as different species in different genera.
- Fig. 12 — *Maternella (M.) cf. empleura* (KUMMEROW, 1939). Right lateral view of a carapace. PS19. IRSNB n° b3769. x80.

PLATE 6

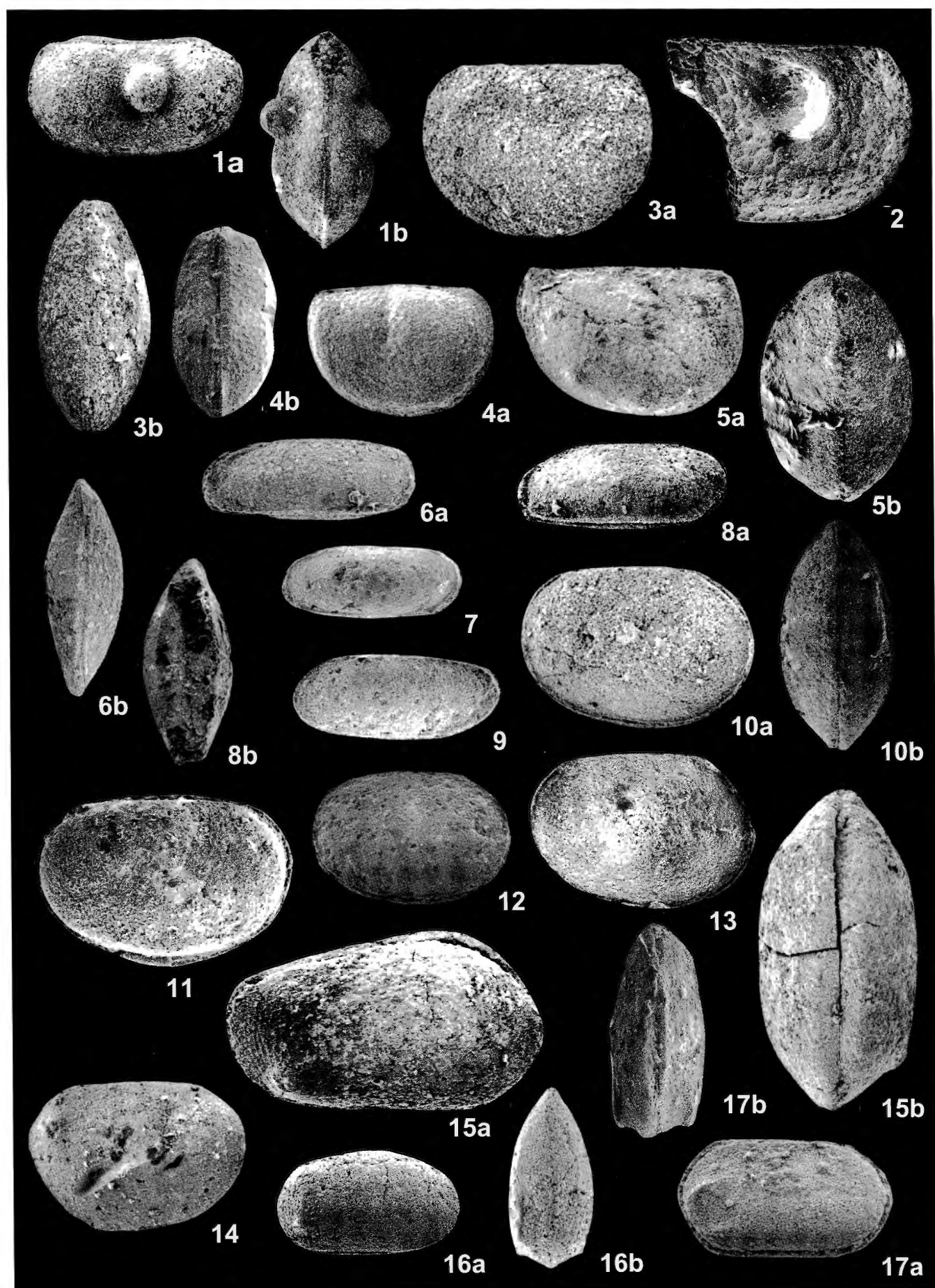
- Fig. 1 — Bioclastic (ammonoid, bivalves, ostracods and trilobite) wackestone. The micritic matrix is not homogeneous due to weak bioturbation. Small black areas consist of ferruginous microbial? tufts dispersed in the matrix. Two geopetal micritic infillings in the right part of the photograph. Préat 56/3, sample 37bis (0,05 m below the D/C boundary), scale bar 600 µm.
- Fig. 2 — Bioclastic (trilobites, molluscs and ostracods) wackestone. The molluscan fragments as well as the matrix contain ferruginous black polyhedral spheroids similar to those of Pl. 7, Figs. 5, 6 and Pl. 8, Figs. 3, 5, 6. Préat 62/8, sample 26 (1,2 m below the D/C boundary), scale bar 240 µm.
- Fig. 3 — Bioclastic (crinoids, molluscs) wackestone with small-sized irregular fenestrae. Micritic matrix of the lower part of the photograph is slightly bioturbated and consists of a very fine-grained calcitic microspar. Abundant ferruginous black spheroids similar to those of Pl. 7, Figs. 5, 6 and Pl. 8, Figs. 3, 5, 6 are present in the micrite and in the microspar. Préat 56/21, sample 42 (0,6 m above the D/C boundary), scale bar 600 µm.
- Fig. 4 — Nodular sponge wackestone-bafflestone with small-sized filiform fenestrae and a larger irregular fenestral cavity on the upper left corner of the photograph. A few ostracods are embedded in the sponge fabric. This latter is an homogeneous very fine-grained calcitic microspar. The nodules are limited by ferruginous and non-ferruginous solution seams. Préat 56/23, sample 53 (2 m above the D/C boundary), scale bar 600 µm.
- Figs. 5, 6 — Slightly bioturbated radiolarian-siliceous wackestone-packstone. Préat 56/10 and 56/11, sample 56 (4,5 m above the D/C boundary), scale bar 600 µm (Fig. 5) and 240 µm (Fig. 6).

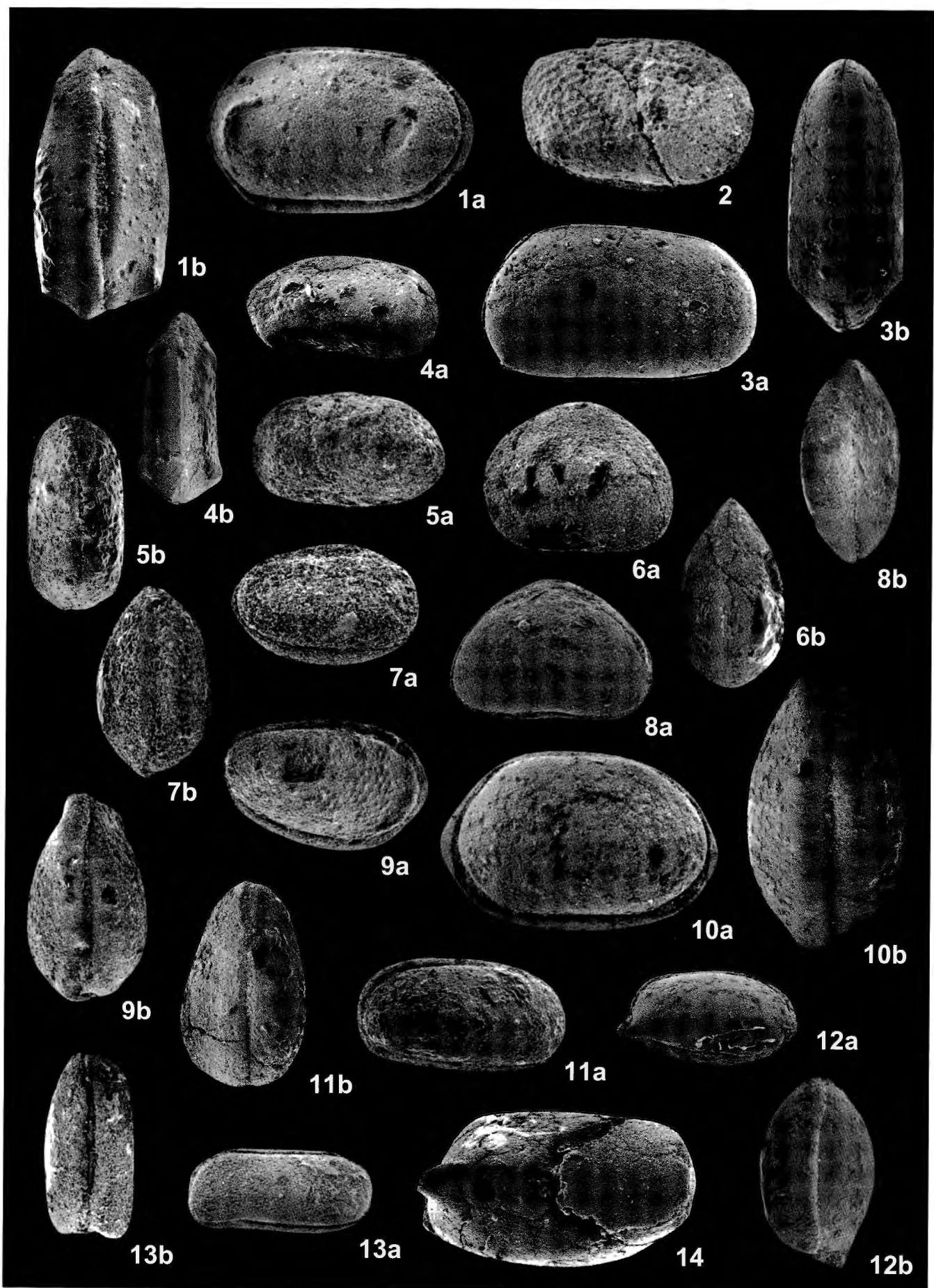
PLATE 7

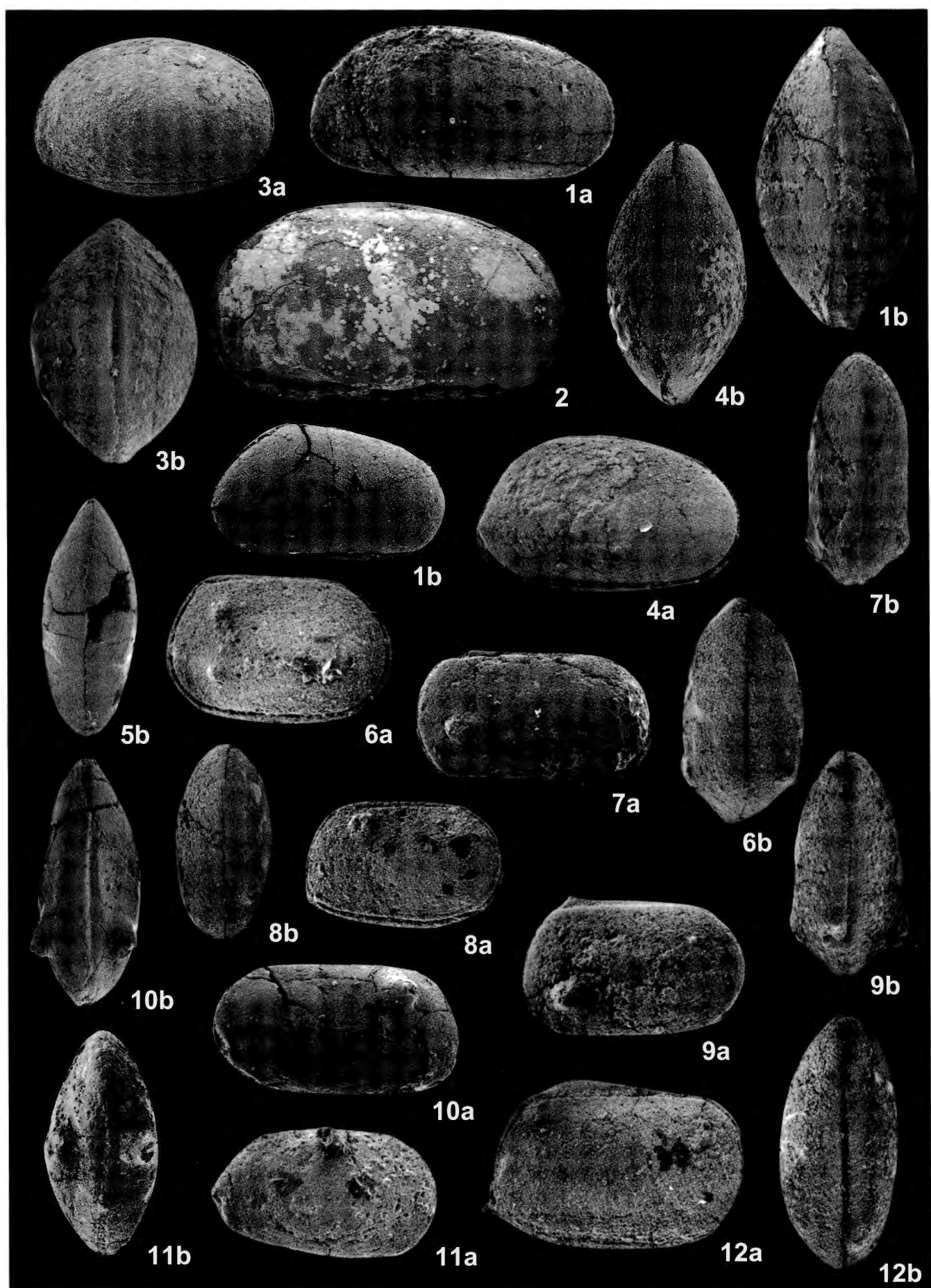
- Fig. 1 — Bioclastic (bivalves and entomozooid ostracods) wackestone. Presence of ferruginous black spheroids similar to those of Pl. 7, Figs. 5, 6 and Pl. 8, Figs. 3, 5, 6. Préat 62/4, sample 10bis (2,3 m below the D/C boundary), scale bar 100 µm.
- Fig. 2 — Ostracod (Entomozoacea) wackestone. The matrix consists of a very fine-grained calcite microspar, forming at a larger scale a typical “clotted” fabric. Préat 62/2, sample 9 (2,8 m below the D/C boundary), scale bar 100 µm.
- Fig. 3 — Thin bioclastic (ammonoids, bivalves, ostracods) packstone layer 4 mm thick in an homogeneous mudstone (not shown here). Ferruginous encrustations around a molluscan fragment and abundant ferruginous black spheroids similar to those of Pl. 7, Figs. 5, 6 and Pl. 8, Figs. 3, 5, 6. The layer is oblique to the stratification, this latter corresponding to the base of the photograph. Préat 56/16, sample 16 (2,2 m below the D/C boundary), scale bar 600 µm.
- Fig. 4 — Burrowed bioclastic (bivalves with one coral fragment on upper part of the photograph) wackestone. The bivalve is encrusted by a thin, discontinuous ferruginous layer of microbial black spheroids. The right vertical of the photograph corresponds to the stratigraphical bottom. Other ferruginous encrustations are present as well as ferruginous microtufts in the micritic matrix (right part). Préat 55/35, sample 36 (0,15 m below the D/C boundary), scale bar 600 µm.
- Figs. 5, 6 — Bioclastic (bivalves, ostracods) wackestone. Irregular ferruginous, cauliflower-like encrustations (microbial blisters) on a recrystallized bivalve. The encrustations include partly or totally microbioclasts (gastropod, ostracods, Fig. 6). The matrix, as well the outer part of the blister contain abundant ferruginous black spheroids. The bottom of the photograph is the stratigraphical base. Préat 54/21 and 54/22, sample 17 (2,15 m below the D/C boundary), scale bar 240 µm (Fig. 5) and 100 µm (Fig. 6).

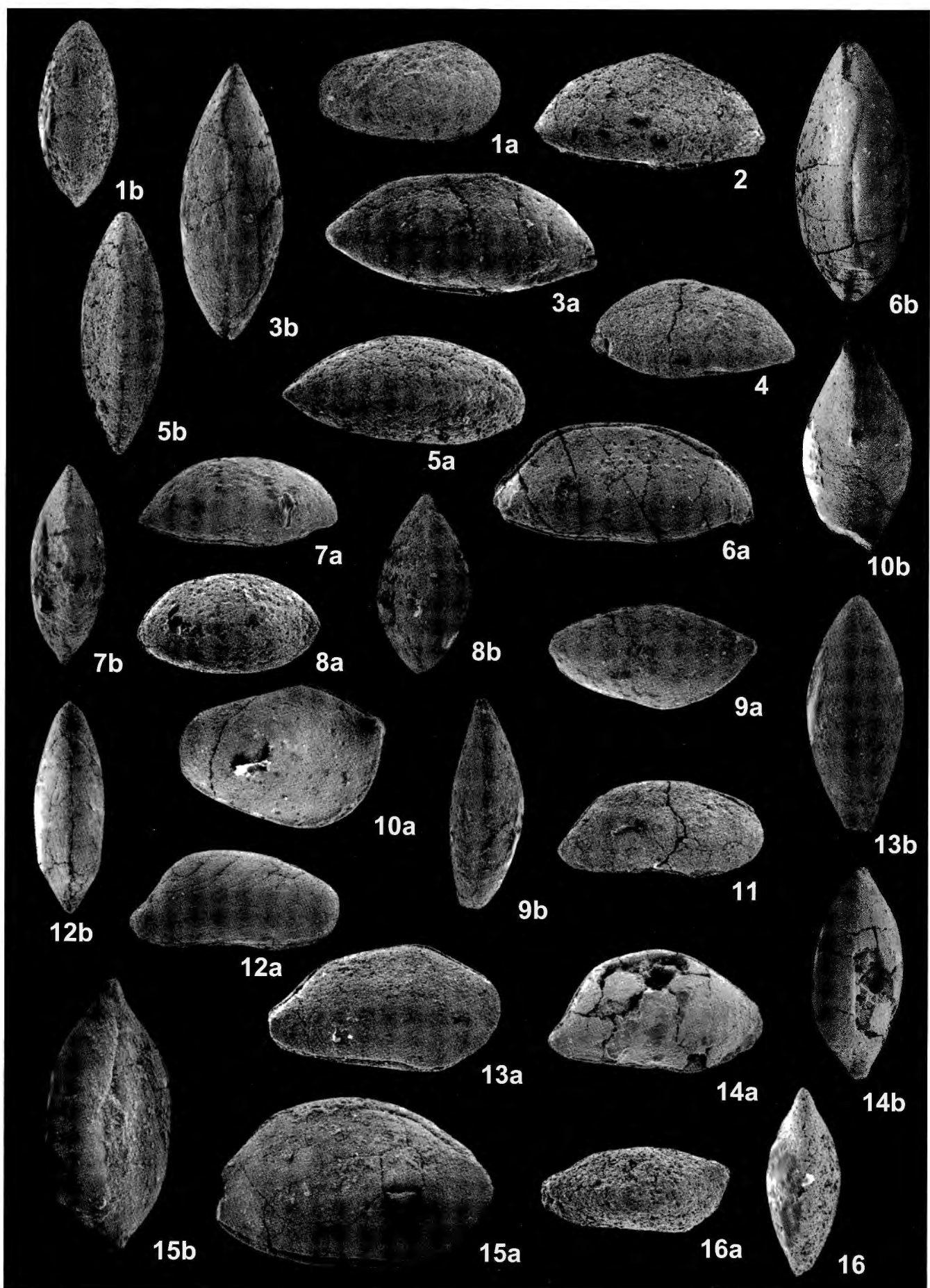
PLATE 8

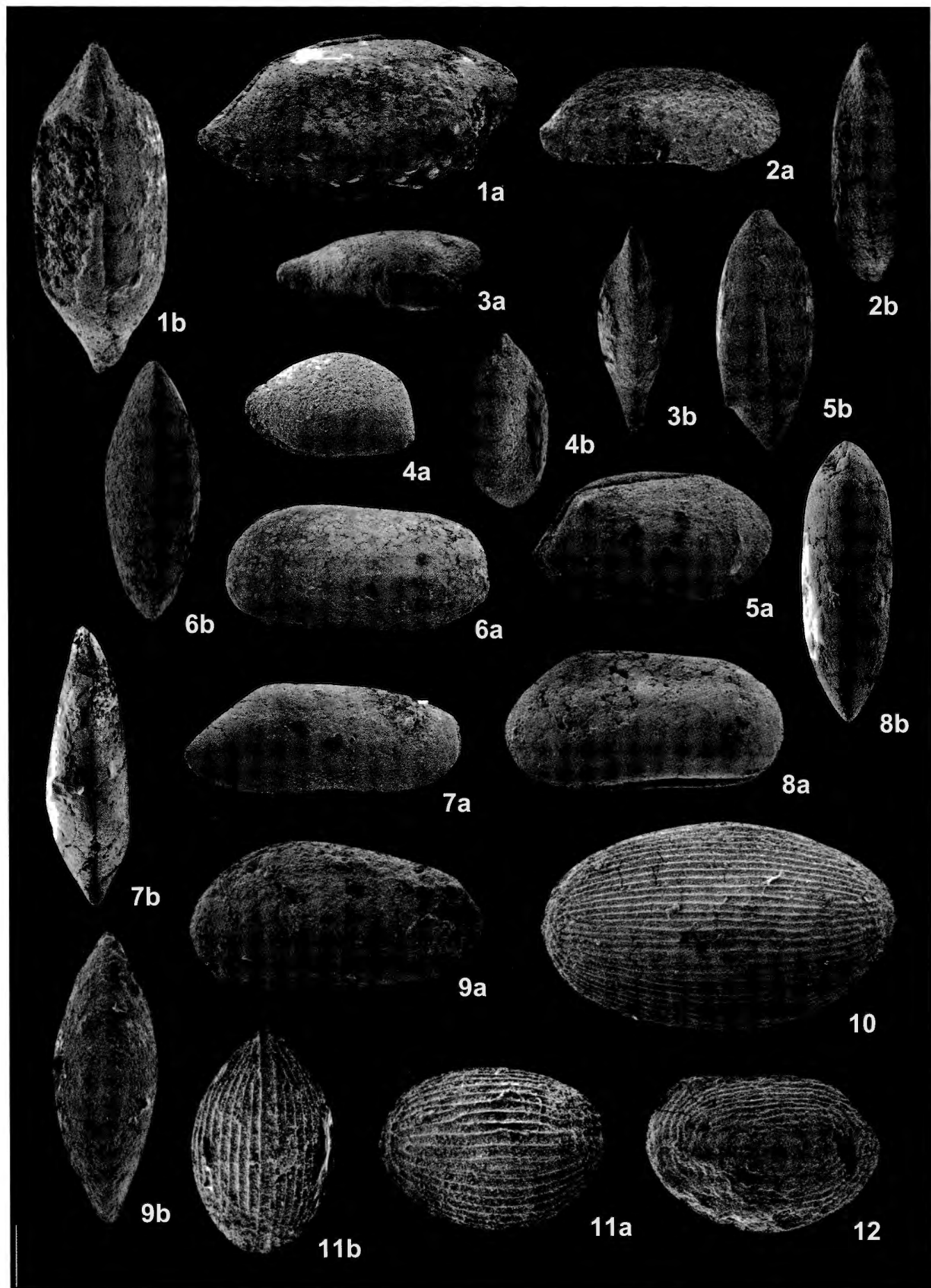
- Fig. 1 — Encrusted bivalve in a bioclastic wackestone containing ferruginous black spheroids similar to those of Pl. 7, Figs. 5, 6 and Pl. 8, Figs. 3, 5, 6. Thick hematite coating on the bivalve displaying ferruginous “dark” irregular sponge borings similar to those of the Devonian Slivenec Limestone (see Mamet *et al.*, 1997). Préat 56/7, sample 41 (0,5 m above the D/C boundary), scale bar 100 µm.
- Fig. 2 — Burrowed bioclastic (molluscs, ostracods) wackestone. “Oncoidal” encrustation of ferruginous black spheroids in the matrix surrounding the bivalve. Ferruginous encrustations are also present directly on the shell. Préat 56/14, sample 10ter (2,35 m below the D/C boundary), scale bar 600 µm.
- Fig. 3 — Ferruginous blister on a small bivalve in a bioclastic wackestone. The matrix contains dispersed, black hematite minerals (spherical and rhombohedral forms) and shows small irregular ferruginous filaments (arrows) as those of Fig. 5, 6, Pl. 8 illustrated from the same sample. Préat 54/23, sample 17 (2,15 m below the D/C boundary), scale bar 100 µm.
- Fig. 4 — Contact between a bioclastic (ostracods) mudstone-wackestone (lower part of the photograph) and a “clotted” wackestone. The clotted fabric consists of a very fine grained greyish (3-5 µm) and coarser (5-10 µm) whitish calcitic microspar. Préat 62/5, sample 10bis (2,3 m below the D/C boundary), scale bar 240 µm.
- Figs. 5, 6 — Ferruginous dichotomic long (up to 300 µm) curved or straight microbial thin filaments (diameter around 5 µm) in a microbioclastic wackestone. Ferruginous black spheroids, polyhedra and rhombohedra (former coccoids?) are associated with the filaments. Préat 54/27 and 54/28, sample 17 (2,15 m below the D/C boundary, scale bar 100 µm (Fig. 5) and 60 µm (Fig. 6).





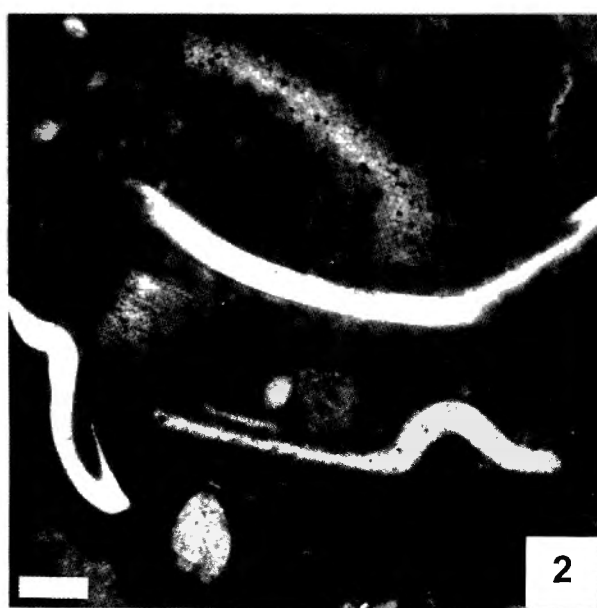




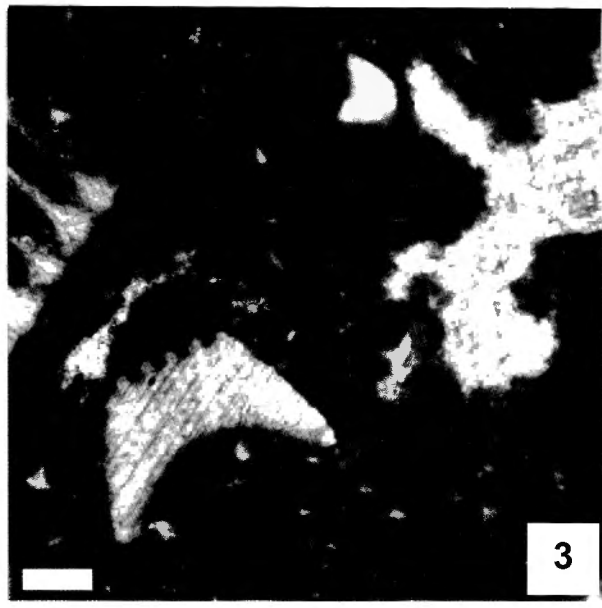




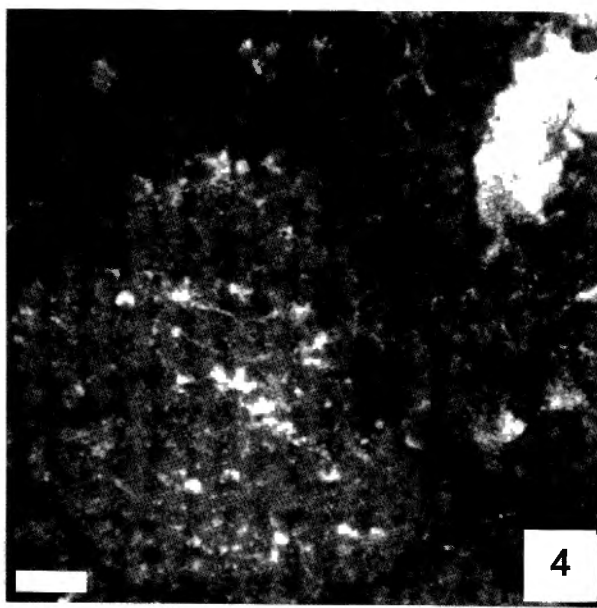
1



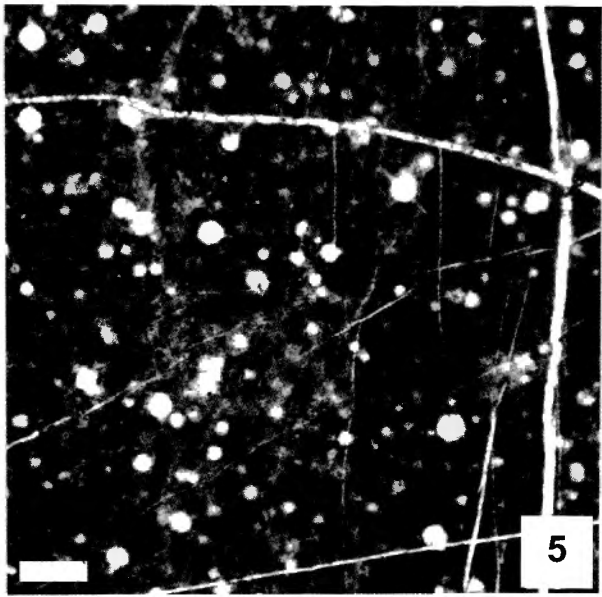
2



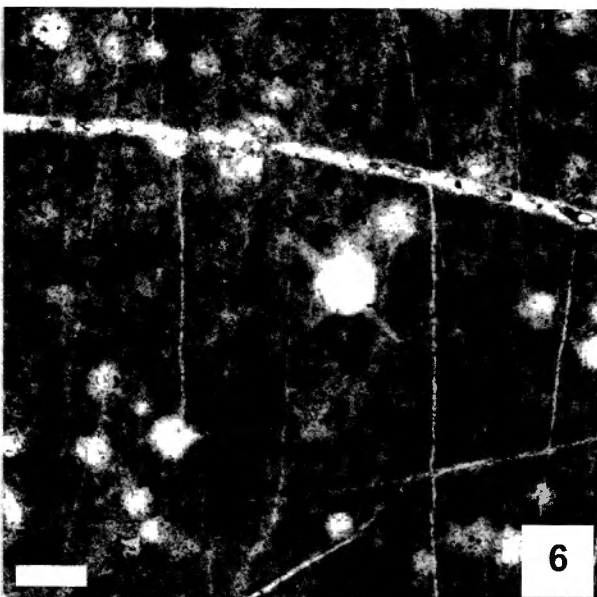
3



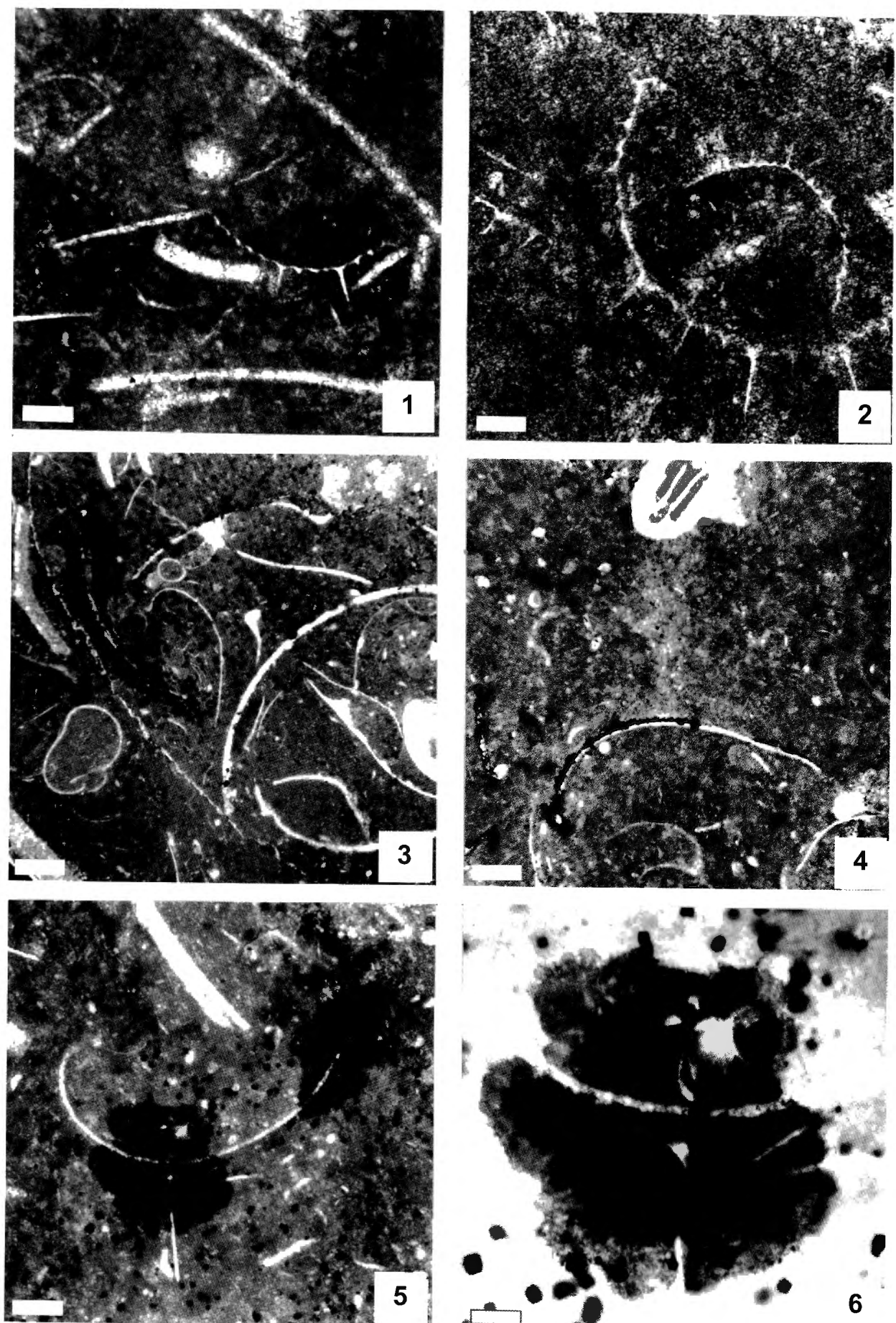
4

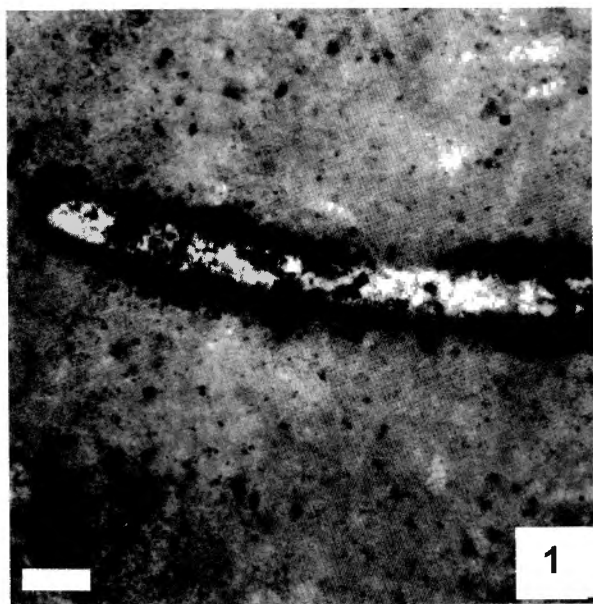


5

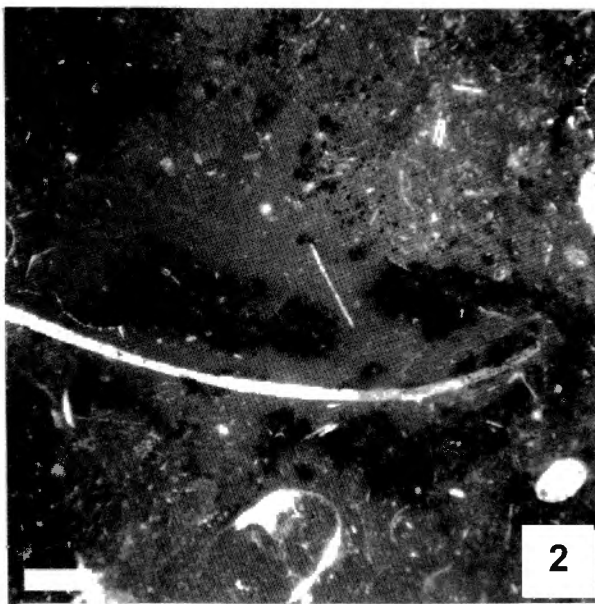


6

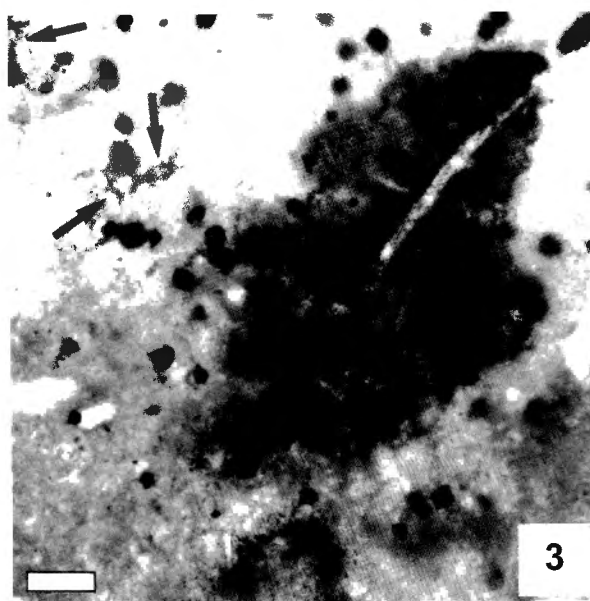




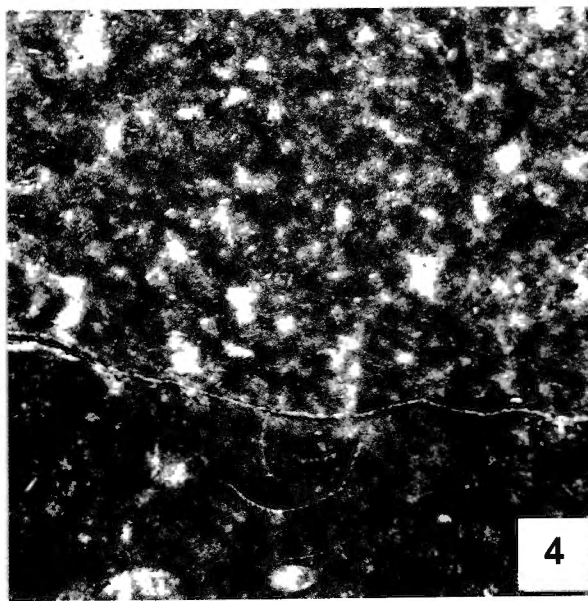
1



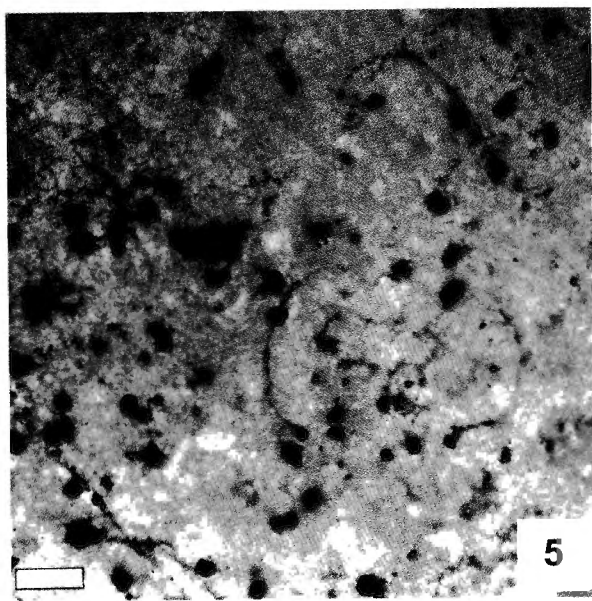
2



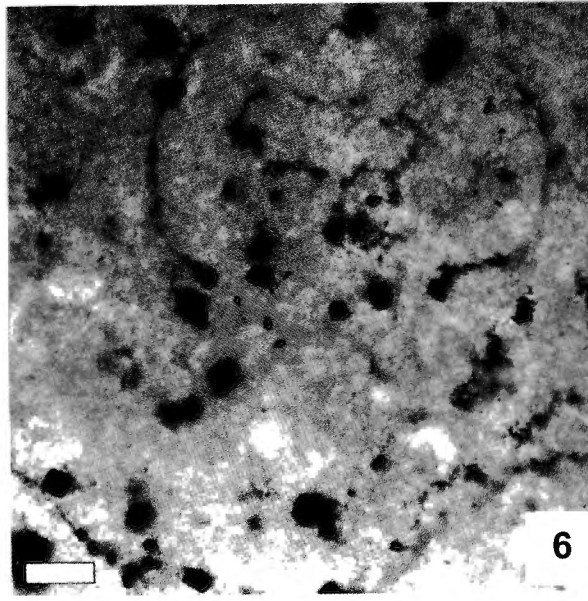
3



4



5



6